Open Journal of Fluid Dynamics, 2024, 14, 24-63
https://www.scirp.org/journal/ojfd
ISSN Online: 2165-3860
ISSN Print: 2165-3852

The Effects of Fluid Sloshing on Different Baffle Configurations in Storage Tanks Transported on Trucks during an Emergency Braking

Che Martin Ayiehfor

Research Unit of Mechanics and Physical Systems Modelling (UR2MSP), Department of Physics, University of Dschang, Dschang, Cameroon
Email: cayiehfor@gmail.com

How to cite this paper: Ayiehfor, C.M. (2024) The Effects of Fluid Sloshing on Different Baffle Configurations in Storage Tanks Transported on Trucks during an Emergency Braking. *Open Journal of Fluid Dynamics*, **14**, 24-63.
https://doi.org/10.4236/ojfd.2024.141002

Received: November 8, 2023
Accepted: February 19, 2024
Published: February 20, 2024

Abstract

Different Baffle designs usable in cylindrical and elliptical storage tanks carried by trucks often used for transporting inflammable liquid materials in Cameroon are investigated to evaluate their safest fluid sloshing damping response during emergency braking where the magnitude of sloshing waves are the greatest. The uncontrolled fluid sloshing creates thrust on the walls of the tanks usually felt externally on the truck carrying the tank and capable of hindering driver's effort to maintain steer ability and improve on safety during critical braking moments. The study first passes through COMSOL, to expose the safest margin of each Baffle type at instantaneous fluid pressure wave propagation initiated at a single phase to reflect sloshing in the storage tank during an emergency braking by the truck carrying the tank. The vivid results can be seen in the domain of Acoustic Iso-surface Pressure response; but also acoustic Pressure and Sound pressure response are seen automatically. Secondly, through an experimental finding in which fluid is forced to pass through each Baffle and the resistance to fluid flow is a measured as it's the Baffle's damping ability. Either, the fluid is lost through the Baffle and by determination of the surface load exerted on each Baffle due to the reaction of the residual fluid acting on the surface of each Baffle after some of it is Lost, the individual sloshing damping abilities are exposed. By comparing the Experimental outcome with the computational response obtained, an ideal Baffle design is proposed for cylindrical and elliptical tanks and considered to respond to abrupt braking more efficiently. The application of the Baffle designs with an average multiple holes rather than the usual face centered proved to be more efficient in fluid sloshing as they provide a more uniformly distributed damping pressure during fluid sloshing in the tank thereby reducing the magnitude of forward thrust that can be created by the conventional Baffle type during emergency braking hence contributing to improving safety. Mindful of the human, material and environmental damages that an accident involving mobile petroleum storage tanks can course, this study is therefore of great significance for design optimization by petroleum storage tank manufacturing companies in Cameroon.

Keywords

Baffles, Loss, Pressure, Sloshing and Iso-Surface

1. Background

The phenomenon of fluid sloshing in mobile storage tanks can be described as a periodic motion of a free surface in partially filled tanks which can be caused by dynamic pitching movements (accelerations and deceleration), rolling seen during cornering or when one side of the vehicle enters a pothole or meet a pump, yawing noticed when a vehicle carrying the storage tank move about the center of gravity may be due to road slip and in a lesser extend Material drainage and cutoff processes. All these phenomena enhance sloshing and this sloshing exerts pressure on the walls of the tank including the baffles such that if enormous, like in the case of an emergency braking, they can create a heavier external thrust on the vehicle which is considered to reduce the ability to maneuvering the vehicle by the driver at that critical moment were safety is needed. The effects of sloshing forces in a tank being towed and on trailers having articulation joints cannot be underestimated. Fluid motion can persist beyond the application of a direct load to the container; the inertial load exerted by the fluid is time-dependent and can be greater than the load exerted by a solid of the same mass. This makes analysis of sloshing very important for mobile storage tanks.

Tanks of different shapes have been used to transport inflammable materials but most common are the cylindrical and elliptical carried horizontally. Be it a truck mounted with an anti-lock braking system (ABS) and electronic stability control system (ESC) working properly, sloshing will still be felt and even more when partially filled. Abrupt deceleration causes the fluid to move to the front of the tank in the direction of forward movement due to momentum. In any unfortunate case of accident, this can be very catastrophic particularly when the tank is occupied by Petroleum volatile inflammable products. History has recorded many accidents linked to trucks carrying tanks in Cameroon. Some include the Yaounde train accidents of 14 February 1998 [1], the Mutegene-Tiko accident of 07 February 2012 [2] claiming lives with lots of material and environmental damages; The trailer accident at Village in Douala on November 17 2021 etc. The images in **Figure 1** below are samples of how dangerous these accidents can be to humans and the environment.

According to the statistics in **Table 1** below from the Ministry of Public Health (MINSANTE), Ministry of Transport (MINT) and Ministry of National

Figure 1. Examples of accidents involving trucks carrying storage tanks for inflammable materials (Source: "Récapitilatif des accidents au Cameroun").

Table 1. Statistics of accidents in Cameroon.

Enrollment in local colleges, 2005		
Year	**Number of Cases**	**Number died**
2019	*165,407*	1290
2020	162,507	930
2021	43,453	200
2022	11,622	372

Source: MINSANTE (Ministry of Public Health).

Year	Number of Accident cases	Number injured	Number died
2016	*2954*	4431	1261
2017	*2341*	3435	929
2018	*1898*	2801	782
2019	*2192*	2313	646
2020	2275	2754	839
2021	2107	2527	963
2022	1833	2068	635

Source: SED (Ministry of Defense).

Year	Number of Accident cases	Number injured	Number died
2017	*6394*	1792	435
2018	*6252*	1759	583
2019	*7199*	1988	513
2020	7303	3097	687
2021	7895	1566	312

Source: DGSN (National Delegation of Security).

security (DGSN and SED) in Cameroon [3], the annual rate of accidents is on the rise and when classifying the various types of vehicles linked to these accidents, up to 18 percent of these accidents involve directly or indirectly heavy-duty trucks transporting materials in storage tanks.

Generally, sloshing waves are initiated in storage tanks by responding through a reaction to an action. The intensity of the response is usually directly proportional to the action particularly if nothing is done in the pathway of the volume of fluid to reduce the reaction as it passes through toward the next surrounding walls. On trucks transporting storage tanks incompletely filled with liquid the effects of this phenomenon may increase during abrupt braking or collision. Baffles are placed inside these tanks to dampen sloshing effects of the fluid and minimize the tendency to create unwanted thrust. The greatest dynamic sloshing surging occurs in mobile storage tanks when partially filled with liquid material. In this light the objective of this piece of work is to investigate and propose the ideal Baffle design that will portray the most efficient damping responses in storage tanks carried on trucks used for transporting liquid materials especially petroleum inflammable products across the national roads in Cameroon.

2. Literature Review

The study of liquid sloshing and Baffles is of great interest to many researchers. Liquid sloshing exploration leads to findings on how the fluid exerts the hydrodynamic forces on the walls of the container and can cause divergence or even damage to the system's functioning [4]. So, the investigation of the hydrodynamic pressure effects on a given Baffles system is necessary.

Between February 2022 to February 2023, we carried out a vivid investigation during internship and field trips in some major producers of cylindrical and elliptical petroleum tanks in Douala Cameroon where almost all of them are located for data collection and industrial experience in petroleum companies in Cameroon. Some of them include the Cameroon Ship Yard (CHANTIER NAVAL), HORIZONE 7, COMETAL SA and METALUX Sarl. By reviewing the design presentation of the baffle implemented in the interior of the tanks by these companies the results were similar all over and **Figure 2** below shows a broken-out view of the current practical dispensation.

In this configuration noted how each Baffle has a parabolic shape with one centralized large hole, one rectangular hole at the bottom and sometimes at the top too. In some cases where I was not allowed to take images, the Baffle design was simply plain surfaces having the same hole patterns as the parabolic type.

Much documentation has been recorded concerning Baffles in storage tanks involving analytic, computerized simulations and experimental approaches. Most of the works on horizontal cylinders are focused on the Eigenvalue sloshing problem, [5] towards the computation of sloshing frequencies and the corresponding modes in the transverse and longitudinal directions. The use of cylindrical

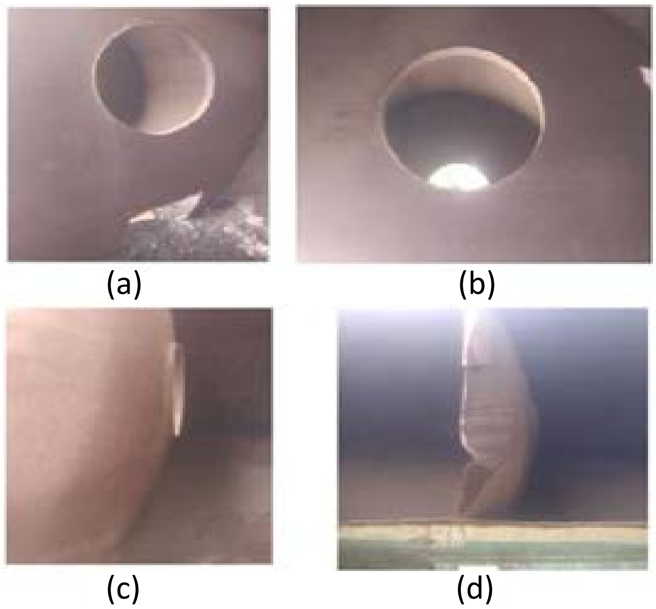

Figure 2. Image of a Baffle in a broken-out Tank (Horizon 7 in Bonaberi).

and elliptical storage tanks used for transporting petroleum products by heavy-duty transport vehicles have been very indispensable ever since petroleum was discovered. A petroleum-carrying storage tank is a medium for storing and transporting materials most often Liquid material. They are a variety of tank shapes but often the circular and elliptical with Baffles insides are commonly mounted on the Automobile chassis to transport liquid materials. The potentials of Baffles in increasing the hydrodynamic damping of sloshing in circular-cylindrical storage tanks has been investigated [6] in which an estimation of hydrodynamic damping ratio of liquid sloshing in Baffled tanks undergoing horizontal excitation was developed analytically using Laplace's differential equation solution. This method involves the assessment of dissipated fraction of total sloshing oscillation energy, which is caused by the flow separation around the Baffles. A series of experiments employing a tank model on a shake table has been carried out to validate the theoretically predicted damping ratio. This parametric study showed that the ring Baffles are more effective in reducing the sloshing oscillations.

There are usually many regulations applied to the design and operation of storage tanks, often depending on the nature of the material it contains. Based on the widespread use of baffles in moving liquid containers, the ability of Baffles to reduce the sloshing effects in storage tanks that are especially broader than fuel containers was under question.

In a more extended study [7], a longitudinal liquid sloshing in partially filled clear-bore tanks causes extensive degradation of tankers' braking performance. To reduce the negative effect of longitudinal liquid sloshing on tankers, three kinds of transverse Baffles were designed, namely, the conventional Baffle, the circular Baffle, and the staggered Baffle. Each kind of Baffle took several forms to investigate the impact of Baffle installation angle, the sizes of holes pierced on the Baffle, and their arrangement on the anti-sloshing effect. FLUENT software was used to simulate liquid sloshing in tanks equipped with different kinds of transverse Baffles and subject to constant braking deceleration. A time-series analysis of the forces acting on tank walls and transverse Baffles was carried out. It was drawn that the Baffle shapes and their installation angle have a great impact on the anti-sloshing effect of Baffles.

According to Amir and Suhash [8], the linearized sloshing problem can be treated as an eigenvalue problem, representing free fluid vibrations inside a container, and provides the sloshing frequencies and modes. Under a specific external excitation, it is converted into a transient problem, representing fluid motion within the moving container. The sloshing solution depends strongly on the container shape. For non-deformable rectangular and vertical-cylindrical containers, the sloshing problem for ideal fluids can be solved analytically, using the separation of variables, resulting in a set of uncoupled equations, one for each sloshing mode.

The regenerative braking force according to Martellucci, L. and Giannini, M. [9] shows that during a significant braking, typical of a Formula Student races, the load distribution on the two axles (front and rear) changes according to many parameters related to the kinematics and dynamics of the suspension system. The pitching movement of the chassis, a function of many parameters (and dive, shock absorbers, barycentric axis, etc.), produces a shift of the vehicle weight towards the front wheels and a corresponding lightening of the rear wheels. The braking phase is therefore particularly complex to analyze and necessarily requires an accurate experimental setup, in consideration of the numerous phenomena that influence its operation. A complete test campaign was then carried out aimed at defining the best setting point for the cylinders of the regenerative braking regulator, measuring the recovered energy, the dynamic behavior of the vehicle and its drivability.

An estimation on the effect of wheel braking of heavy trucks (13 and 20 tons per axle) on the deformations observed in the braking zones (traffic lights, roundabouts) was conducted by [10]. For this purpose, two pavements of the city of Ouagadougou (National Road 1 and National Road 2) differing by the geometrical values and the nature of the materials used for the formulation of the pavement layers were studied. The static braking mechanism under extreme heat wave conditions was simulated using Comsol Multiphysics 5.2 software in order to evaluate the values of the temperature that could be observed. A comparative study of the simulated temperature values at the surface of the wearing courses of these pavements with the melting temperatures of the bitumens was carried out for the selected loads.

3. Theory

3.1. Sloshing and Surging Phenomenon in Mobile Fuel Tanks

Most dynamic sloshing and surging occur in mobile storage tanks carried on

Lorries particularly when partially filled with fluid [11]. It should be noted that even small fuel tanks of passenger cars also have Baffles and experience these phenomena thus are fitted with internal Baffles to minimize fuel movements. Figure 3 and Figure 4 below show the behavior of fluid in a mobile storage tank during pitching (acceleration and deceleration) yawing and rolling.

The momentum created by these behaviors increases the uncontrollability of the driver thereby increasing the risk of accidents, disasters and failures. Furthermore, Most storage tanks with perforated holes on the Baffle experience some sort of fluid flow phenomenon. The passage of fluid through the Baffles from one compartment to another during sloshing wave is via the hole which leads to the understanding of fluid presentation at a given moving speed after the Baffle in relation to Renaults number.

(Re) given by:

$$\mathrm{Re} = \frac{\sigma v D}{\mu} \tag{1}$$

where:

ρ = Density of Fluid

v = speed of fluid flow

D = Diameter of hole

μ = dynamic viscosity index

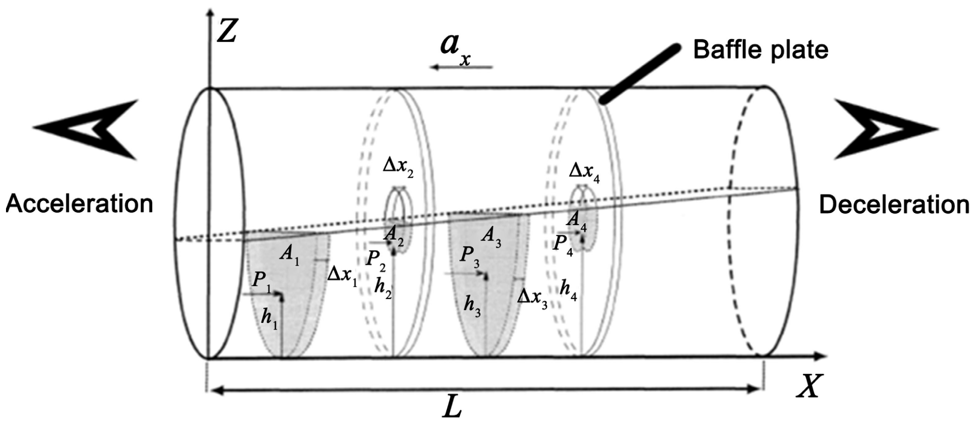

Figure 3. Sloshing phenomenon in a mobile Tank during acceleration and deceleration [12].

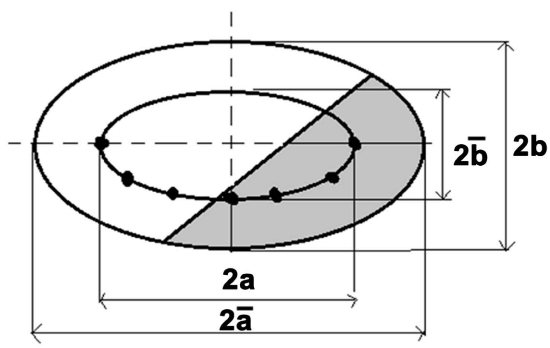

Figure 4. Sloshing phenomenon in a mobile Tank during Rolling and Yawing [12].

A section of a hole viewed at microscopic level is a cylinder or pipe and therefore, depending on the finishing aspect inside the walls of the hole and the speed of fluid flow, it is possible to get turbulence if the Renaults number (Re) is greater than 4000 or Transitional if the Re lies between 2300 - 4000, and laminar if Re is less than 2300 [12]. **Figure 5** below shows an illustration of the various flow phenomena through a Baffle hole in relation to Re.

3.2. Safe Working Pressure in Tanks

While designing any new vessel and equipment, the creators have to keep many things in mind. Before starting the design of these vessels, the engineers have to check their design pressure. After completing the design, they have to check for maximum allowable working pressure (MAWP) and maximum allowable operating pressure (MAOP) [13]. The importance of these calculations is that they help in increasing the quality and durability of the product. MAWP of the vessel depends on thickness, the material used for its construction and operating temperature. At maximum allowable working pressure, the vessel portrays its optimal performance. However, the MAWP keeps changing with time as the vessel might sometimes get corroded or fatigued.

Before calculating for MAWP, process engineers need to determine the size, shape, and required psi of a vessel, as well as the physical properties of the desired metal alloy. By doing so, the vessel can be constructed with the right structural materials and thickness to meet the calculated MAWP. Alternatively, the MAWP can be calculated for a variety of standard pressure vessels so the right vessel can be selected and added to an industrial facility system.

Once MAWP is determined, the vessel is hydrotested *i.e.*, filled with pressurized water at the established MAWP to verify that the vessel can handle the pressure.

The American Society for Mechanical Engineers [14] establishes the standards for the design and construction of pressure-rated vessels, including acceptable MAWPs. Their established formula for calculating a vessel's MAWP is as follows:

$$P = \frac{\sigma t E}{Rs} \quad (2)$$

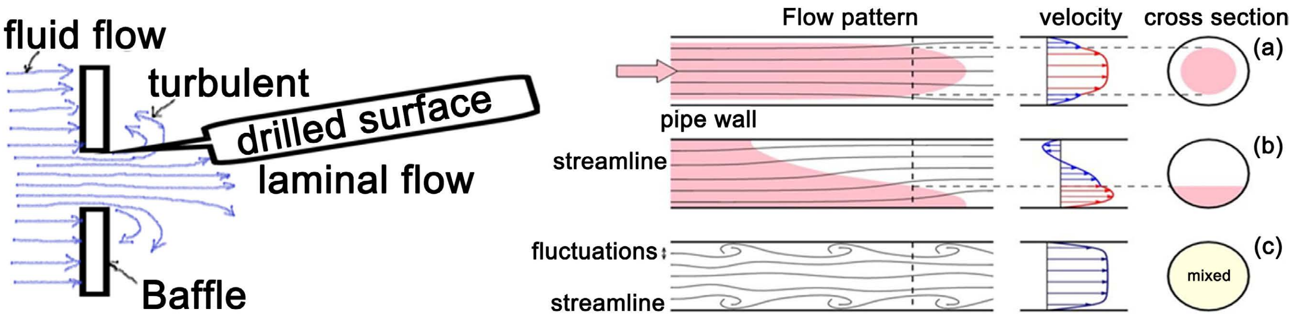

Figure 5. (a) Fluid behavior around a Baffle hole, (b) Laminar and turbulence phenomenon in relation.

whereby:

P = Maximum allowable working pressure (in Pa)

σ = tensile strength of the material in the weakest part of the vessel (in psi)

t = Vessel's wall thickness (in mm)

E = Longitudinal seam efficiency, or efficiency of the weld based on a set rating R = Interior radius of the vessel (in mm)

s = Safety factor

Mindful of the fact that the maximum speed limit for trucks in Cameroon is 60 km/h, it is estimated that a truck carrying a storage tank moving at this speed and carrying its maximum allowable load can take at least 5 seconds to come to a standstill during an emergency braking given that all favorable conditions are applied including good road quality, functional ABS and steadily applied braking. During such instances, fluid sloshing intensifies and the unsafe working pressure in the tank is approached particularly if it is partially filled.

4. Methods

4.1. Computerizes Method

The focus here is to expose the safest margin of each Baffle type at instantaneous fluid pressure wave propagation initiated at a single phase to reflect sloshing in the storage tank during emergency braking where an unsafe working pressure can be experienced by the Truck carrying the tank. The vivid results seen in the domain of Acoustic Iso-surface Pressure response; but also Acoustic Pressure and Acoustic Sound pressure response are seen automatically. Problem of partially filled tank necessity that we have to take the combination of fluid plus the structure in which it is filled thus making the problem purely Fluid and structure interaction. This type of problem can be modeled in basic four approaches [15] which are used for fluid-structure interaction problems including, Lagrangian approach, Euler approach, Euler and Langrangian approach. The Lagrangian formulation is usually used for describing a solid mechanics problem. The problem is described with a high number of mass particles, where the motion of every single particle is being observed in space and time. The problem is exactly defined when the motion of all the particles is known. The Lagrangian formulation is very simple and easy to use for one or only a few mass particles. However, the method becomes very complicated and complex for description of high number of mass particles. In the Eulerian formulation, the problem is being observed at one point in space which does not follow the motion of the single particle. In one time step t several mass particles may pass the observed point. Their motion is exactly determined in the moment of passing through the observed point knowing the field variables are time dependent.

The application of COMSOL to sort out these findings makes use of the main parametric model of acoustics in the frequency domain the Helmholtz equation. The model involved is the cylindrical and elliptical storage tanks with their geometries presented below (**Figure 6**).

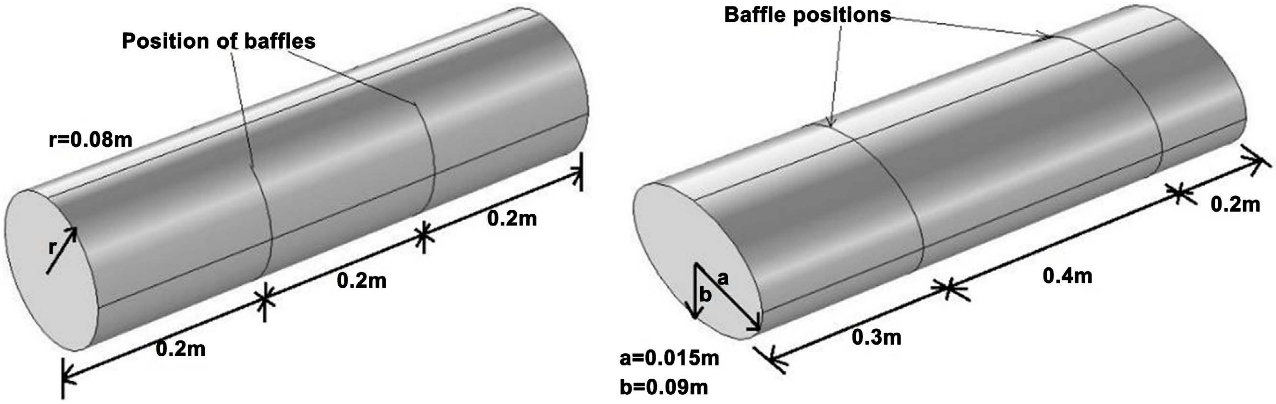

Figure 6. Cylindrical and elliptical tanks are under study.

Because the Helmholtz PDE is a time independent PDE it can be solved more efficiently compared to the time dependent wave equation used for modeling acoustics in the time domain. The Helmholtz equation is, however, only applicable when modeling acoustic systems which have a harmonic time dependency.

All these analyses are based on the Helmholtz PDE model in conjunction with various types of boundary conditions. The provision of a time harmonic analysis let to the computing of the frequency response of an acoustic system over a range of frequencies for different baffle configurations. Note should be taken that an eigenfrequency analysis is applied to solve for the eigenmodes and eigenfrequencies of an acoustic system. The designing of the various Baffles for the cylindrical tank was with respect to a parametric study carried out by Abbas and Ziyaeifar (16) which led to the uprising of the following partitioning on various circular Baffle. (**Figure 7**)

On the other hand, the various Baffle designs placed under study in the elliptical tank were obtained through design modeling and testing on the software while considering the surface area and structural rigidity performance to obtain optimal performance. The model below was considered, then by eliminating one hole at a time the remaining surface structure was simulated. (**Figure 8**)

Acoustic pressure is the main quantity that characterizes acoustic fields since most acoustic-sensitive items such as the ear are pressure sensitive. The pressure-wave propagation in a tank is a measure of sloshing dynamics phenomena in the tanks. The approach is general for analysis of damping of harmonic pressure waves. The test model involved here is geometry consisting of three separate chambers divided by Baffles. The inlet and the outlet correspond to the movement of fluid during braking due to the force of inertia and in connection to the direction of movement of the vehicle carrying the tank.

4.1.1. Helmholts Equation

The behavior of an acoustic system in the frequency domain is investigated by repetitively solving the Helmholtz PDE for a specific frequency out of a frequency range of interest. The Helmholtz equation is used for modeling a harmonic sound pressure field at a specific angular frequency ω:

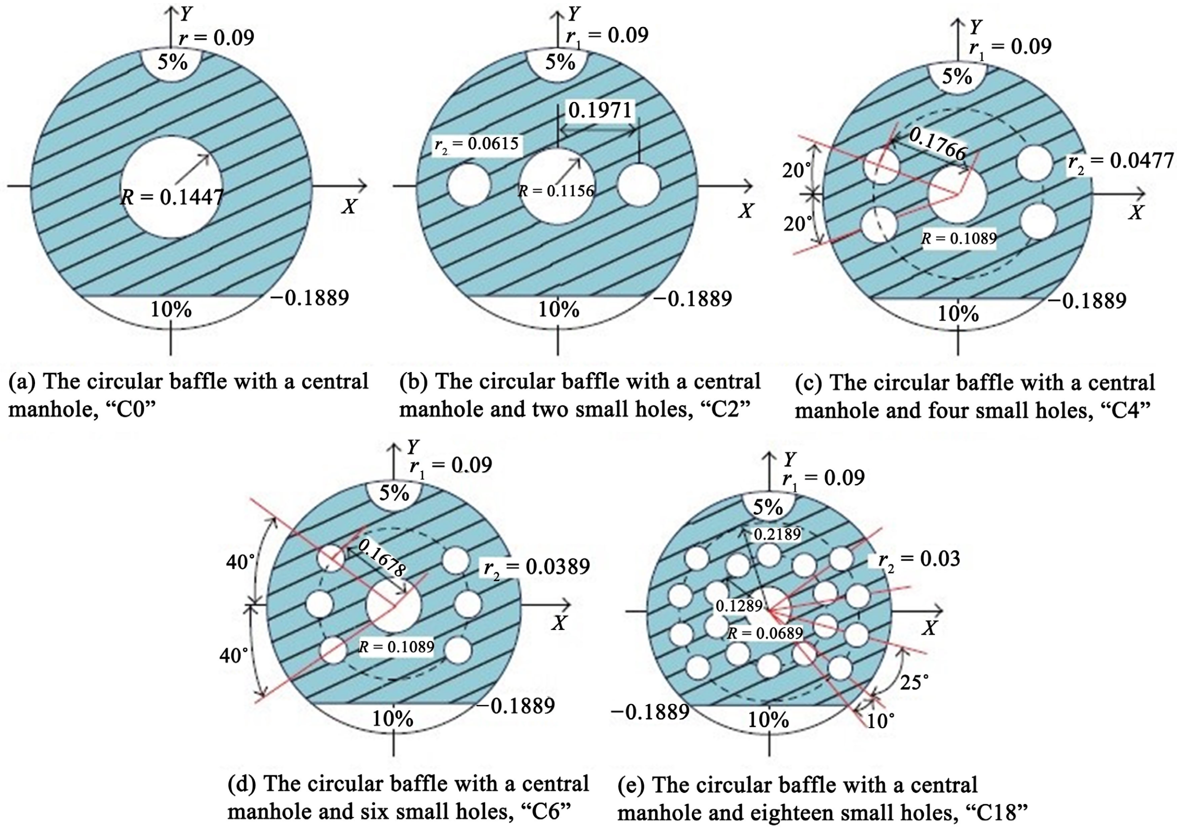

Figure 7. Various Baffles designs for cylindrical tanks [15].

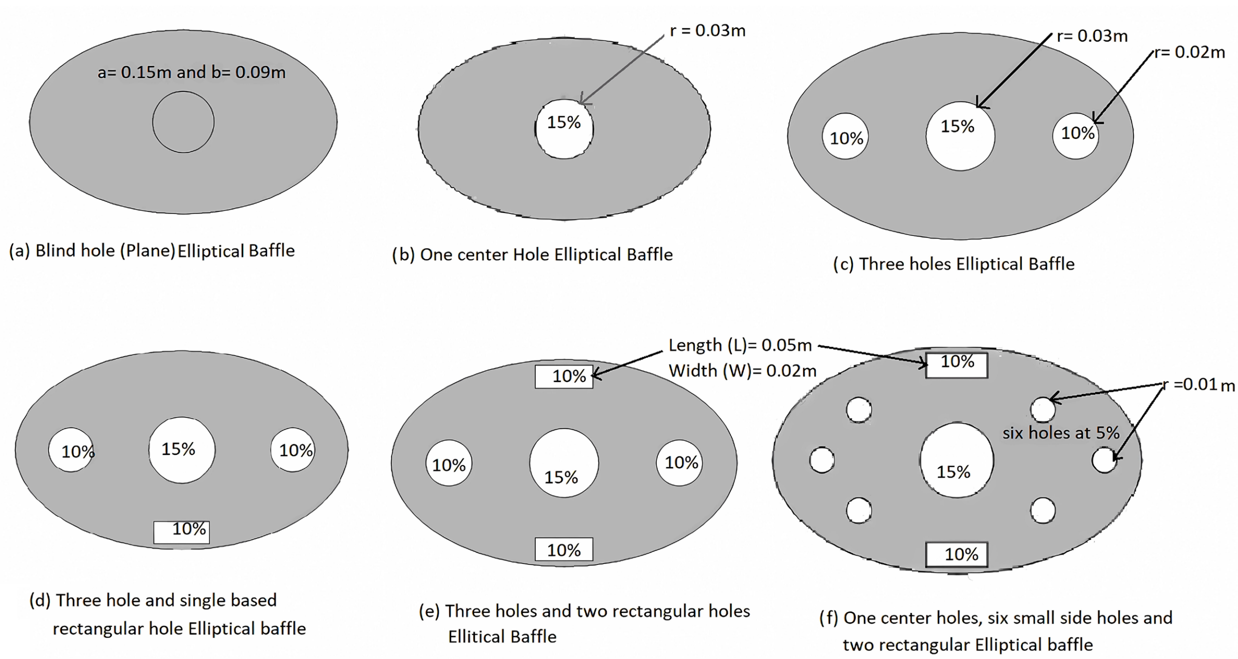

Figure 8. Various Baffles designs for elliptical tanks.

$$\nabla \cdot \left\{ -\frac{1}{\rho} \left(\nabla p(x) + F \right) \right\} - \frac{\omega^2}{\rho c^2(x)} = 0 \tag{3}$$

The Helmholtz equation is derived from the wave equation with harmonic time-dependence.

Here the terms $Q(t, X)$ and $F(t, X)$ are monopole and dipole sources, respectively.

Thus, if a sound pressure field is assumed to be time-harmonic, the pressure variation in time for a particular frequency ω can be expressed in the complex plane by an amplitude function $p(X)$ such that:

$$p(t,X) = p(X)\mathrm{e}^{iwt}$$

Likewise, the monopole and dipole sources can be expressed by amplitude functions $Q(X)$ and $F(X)$, respectively:

$$p(t,X) = Q(t,X)\mathrm{e}^{iwt}$$

$$F(t,X) = F(X)\mathrm{e}^{iwt}$$

Taking the second order time derivative of (1) gives:

$$\frac{\partial^2 p(t,X)}{\partial t^2} = \nabla p(X)\mathrm{e}^{iwt} \tag{4}$$

Taking the gradient yields to

$$\nabla p(t,X) = \nabla p(X)\mathrm{e}^{iwt}$$

$$\frac{1}{pc^2}\frac{\partial^2 p(t,X)}{\partial t^2} + \nabla\cdot\left\{-\frac{1}{\rho}\left(\nabla p(t,X) + F(t,X)\right)\right\} + Q(t,X) \tag{5}$$

Thus inserting the above in the main equations gives

$$\nabla\cdot\left\{-\frac{1}{\rho}\nabla p(X)\mathrm{e}^{iwt}\right\} - \frac{\omega^2}{\rho c^2(x)\mathrm{e}^{iwt}} = Q(X)\mathrm{e}^{iwt} \tag{6}$$

Factor out the common term then the equation simplifies to the time-independent, inhomogeneous Helmholtz equation as follows:

$$\nabla\cdot\left\{-\frac{1}{\rho}\left(\nabla p(X) + F\right)\right\} - \frac{\omega^2}{\rho c^2(x)\mathrm{e}^{iwt}} = Q \tag{7}$$

The dependent variable in the Helmholtz equation is the sound pressure p. The sound pressure wave is propagating in a medium with density at the speed of sound c. The sound pressure field is modeled in response to a harmonic sound stimulus at a frequency f, which is related to the angular frequency ω by: $p(X) = \frac{\omega}{2\pi}$. Sound pressure can be understood as the local pressure deviation from an ambient reference pressure: $p(X) = P_{\text{medium}}(X) - P_{\text{reference}}$ where X denotes the position vector. Terms Q and F represent monopole and dipole sources, respectively.

4.1.2. Domain of Equation

In solving problems in the frequency domain using the Pressure Acoustics interface in COMSOL software, the model equation is a slightly modified Helmholtz equation for the acoustic pressure, p

$$\nabla \cdot \frac{\nabla p}{\rho} - \frac{\omega^2 p}{c_s^2} = 0 \tag{8}$$

where ρ is the density, c_s is the speed of sound, and ω is the angular frequency. The density needs to be included in the equation in cases where variations in density in different materials exist. The model assumes that in the low-frequency range, reactive damping prevails. Resistive damping is therefore not included.

4.1.3. Boundary Conditions

The boundary conditions are of three different types. At all the solid boundaries, which include the outer walls of the tank, the dividing walls between the resonator baffles, and the walls of the perforated holes, sound-hard (wall) boundary conditions are used. This is such that:

$$\left(-\frac{\nabla p}{\rho}\right) \cdot n = 0 \tag{9}$$

At the inlet boundary is a combination of incoming and outgoing plane waves

$$\left(-\frac{\nabla p}{\rho}\right) \cdot n = \frac{i\omega}{\rho c_s} p - \frac{2i\omega}{\rho c_s} p_0 = 0 \tag{10}$$

In this equation, p_0 denotes the applied outer pressure and i the imaginary unit. At the outlet boundary, an outgoing plane wave is set.

$$\left(-\frac{\nabla p}{\rho}\right) \cdot n = \frac{i\omega}{\rho c_s} p \tag{11}$$

This above scientific analysis has led to many studies to bring about improvement on its development and use. One of them is the following results to amelioration tank interior designs with the target part of the tanks to be studied critically being the baffle designs placed in the tanks to improve on its functionality.

4.1.4. Results and Discussion of Simulations

The simulation results presented in this section are based on the solution of the truncated systems built in the air. The same test was conducted for fluids like water and liquid petroleum products embedded in the COMSOL software configuration [17] where the iso-surface pressure proved to be the same as in build-in air for the same harmonic and frequency excitation. The results for the Eigenvalue problems are based on the in-built solution to systems.

The eigenvalue problem is considered first with respect to Sloshing Frequencies, Modes, and Masses, the frequency is at 1000 Hz. Thus assuming there is no external excitation. The convergence rate and the expected accuracy of the eigenvalues are demonstrated numerically [19] [20] [21], increasing the value of truncation size leading to the particularities as seen in these results.

The following images (**Figures 9-20**) are the results of the computerized study.

Here more attention should be on the iso-surface pressure results shown on bottom left hand and the graph of lost with respect to sloshing responds for each configurations of holes on the Baffle shown on the bottom right of each image.

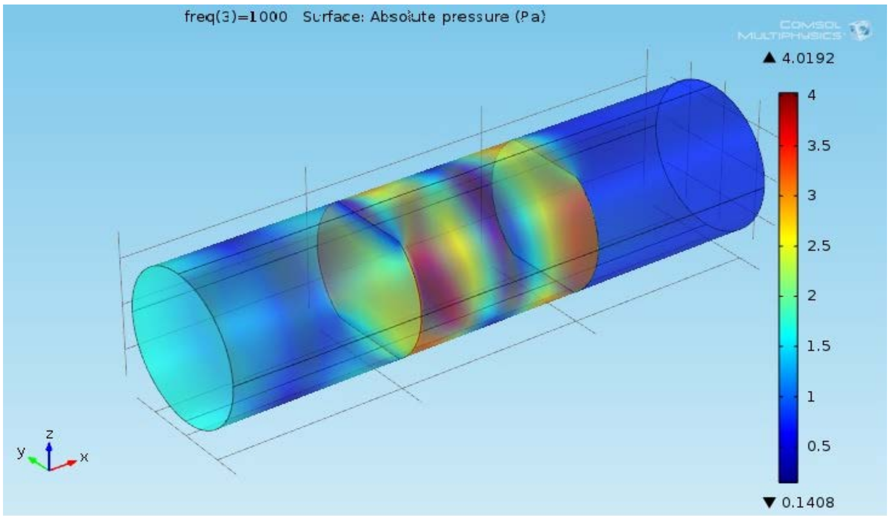
freq(3)=1000 Surface: Absolute pressure (Pa)
▲ 4.0192
4
3.5
3
2.5
2
1.5
1
0.5
▼ 0.1408
z
y
x

(a)

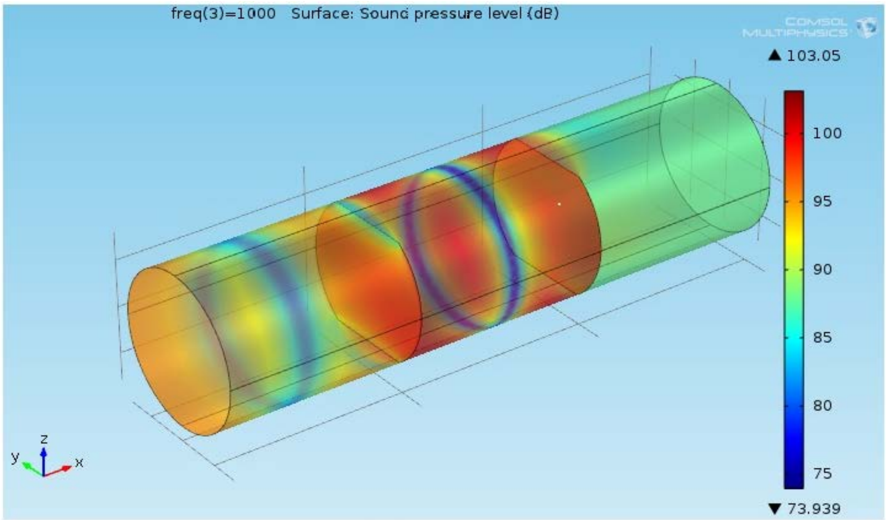
freq(3)=1000 Surface: Sound pressure level (dB)
▲ 103.05
100
95
90
85
80
75
▼ 73.939
z
y
x

(b)

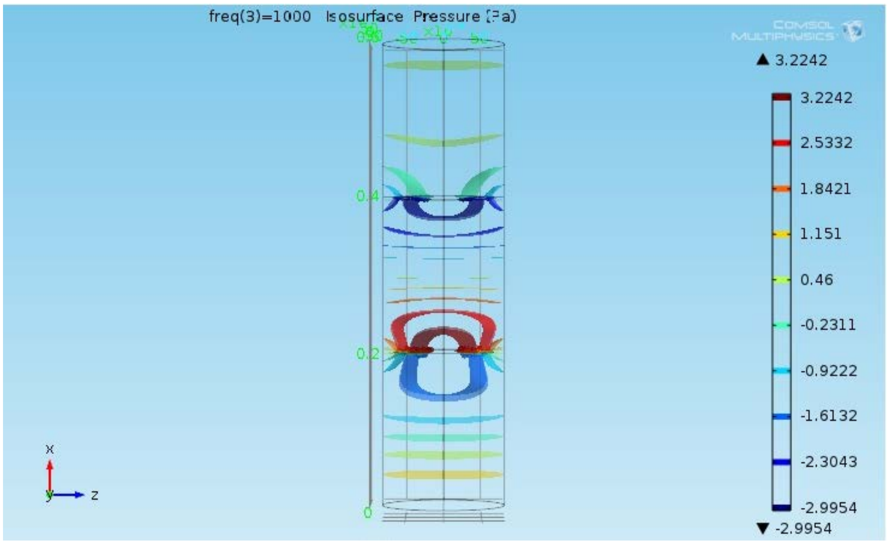
freq(3)=1000 Isosurface: Pressure (Pa)
▲ 3.2242
3.2242
2.5332
1.8421
1.151
0.46
-0.2311
-0.9222
-1.6132
-2.3043
-2.9954
▼ -2.9954
0.4
0.2
0
x
z

(c)

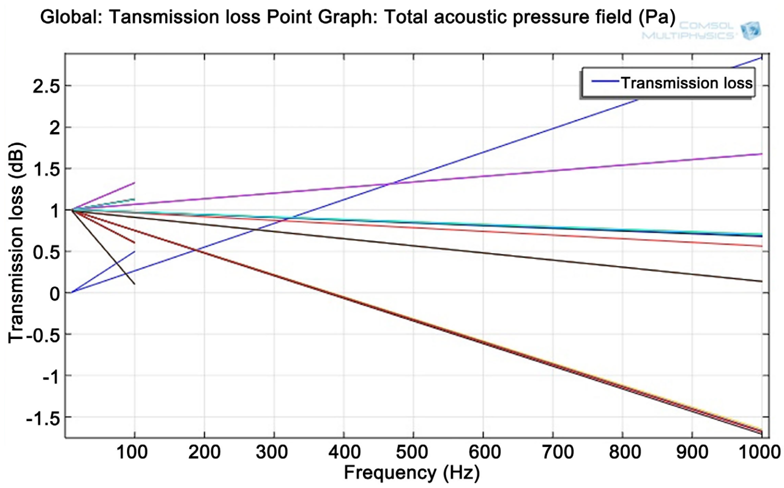

(d)

Figure 9. Conventional Baffle in cylindrical tank, (a) Acoustic pressure field, (b) Surface sound pressure, (c) Iso-surface pressure, (d) Transmission loss and point graph of total acoustic pressure.

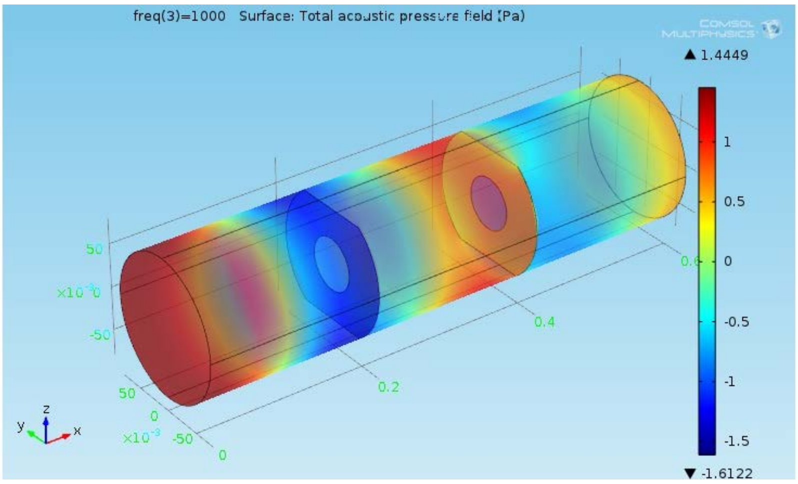

(a)

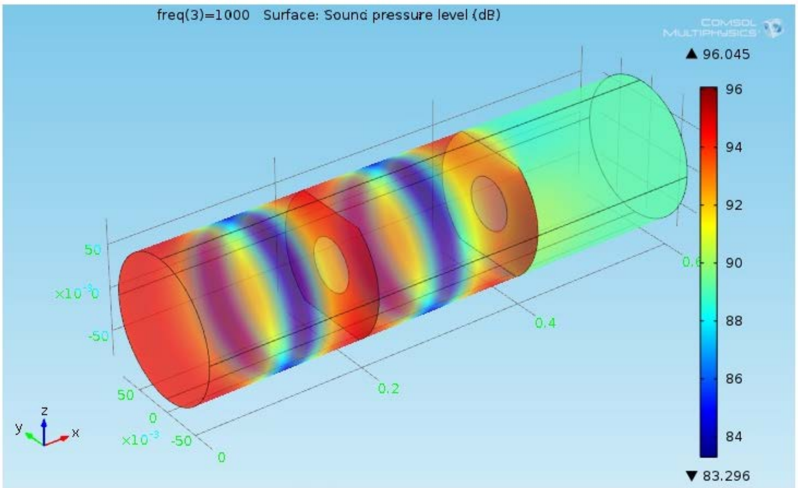

(b)

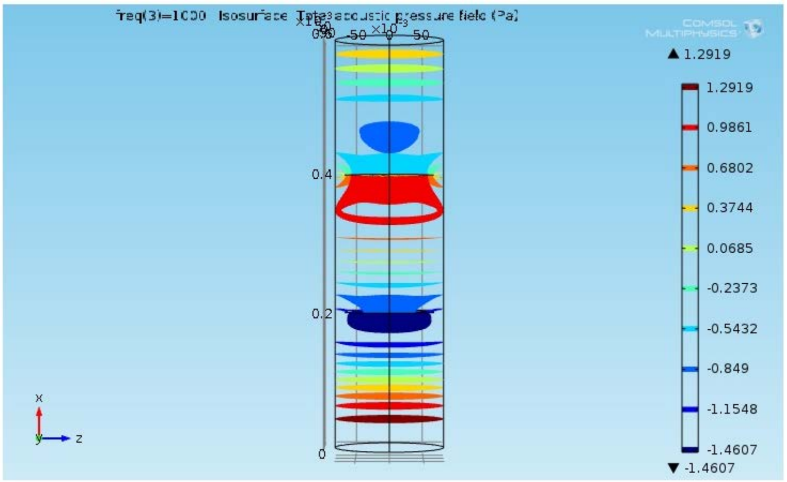

(c)

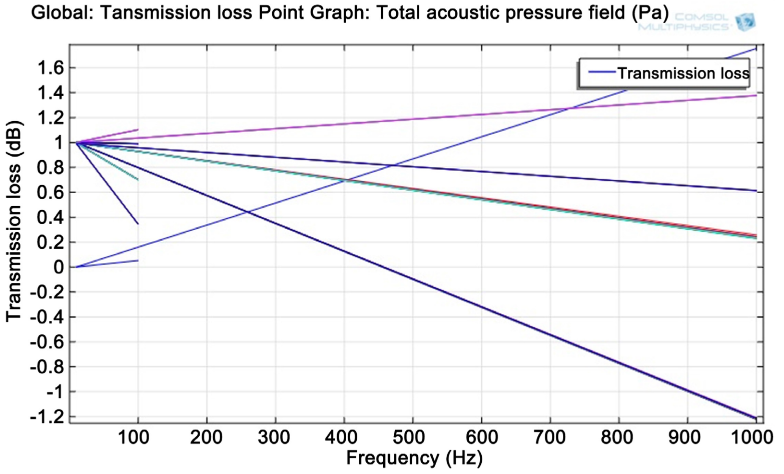

(d)

Figure 10. Conventional Baffle with a center hole (manhole) in a cylindrical tank. (a) Acoustic pressure field, (b) Surface sound pressure, (c) Iso-surface pressure, (d) Transmission loss and point graph of total acoustic pressure.

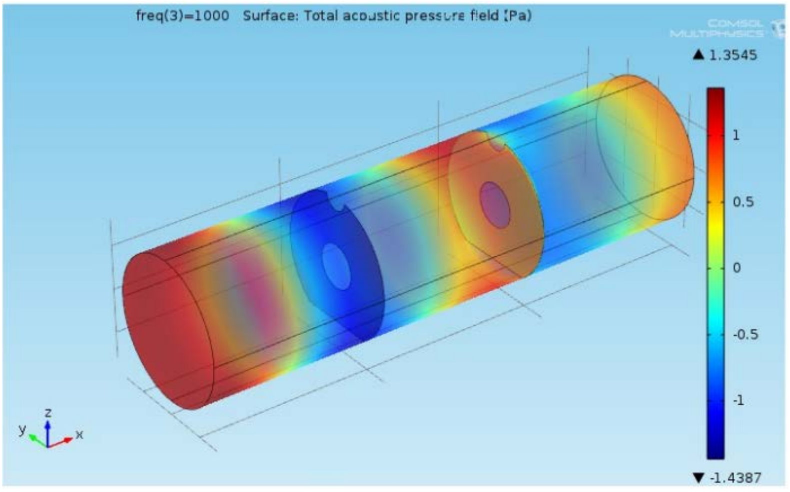

(a)

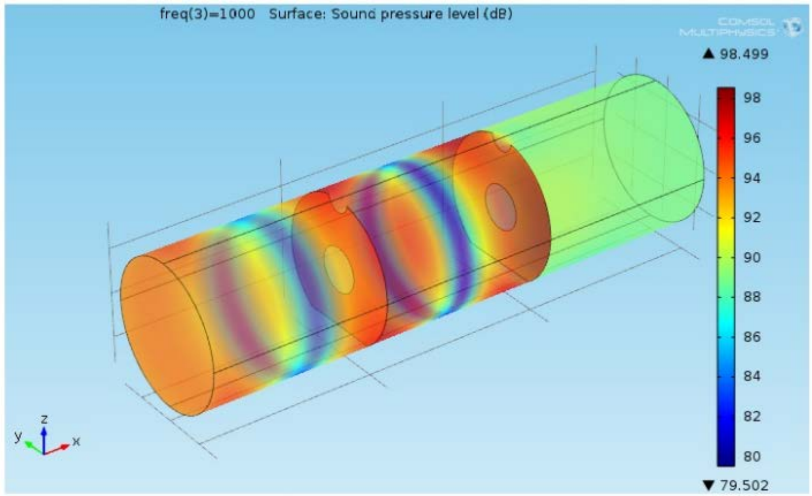

(b)

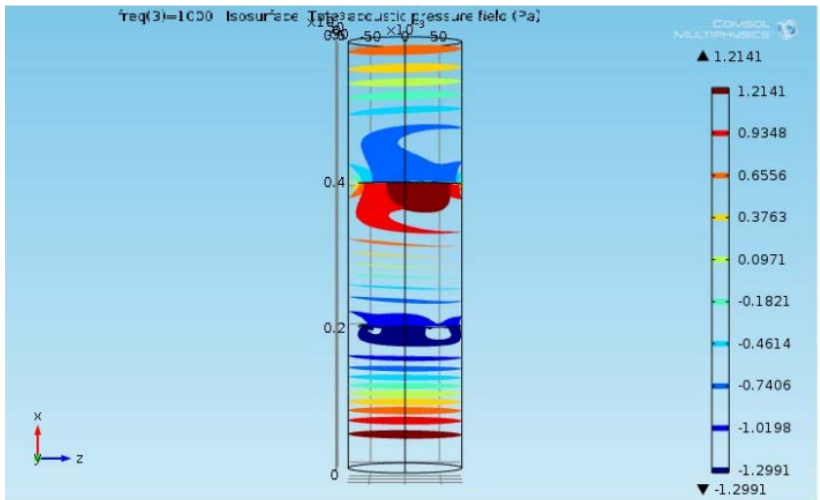

(c)

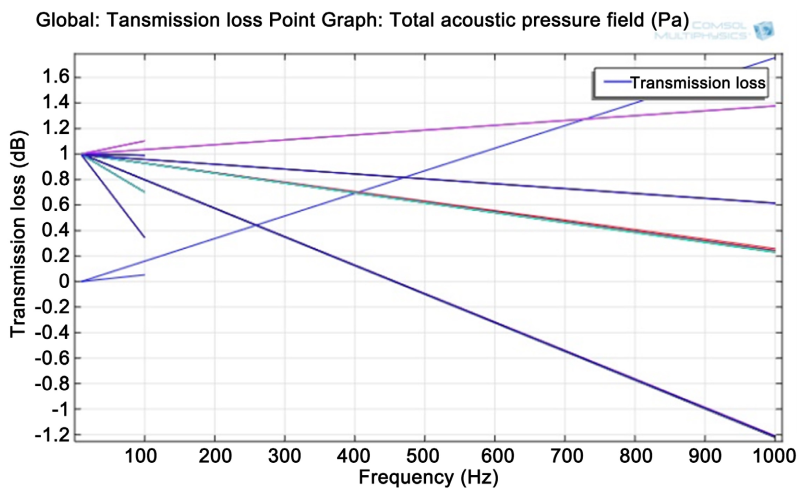

(d)

Figure 11. Conventional Baffle with one center hole (manhole) and one sector hole in a cylindrical tank: (a) Acoustic pressure field, (b) Surface sound pressure, (c) Iso-surface pressure, (d) Transmission loss and point graph of total acoustic pressure.

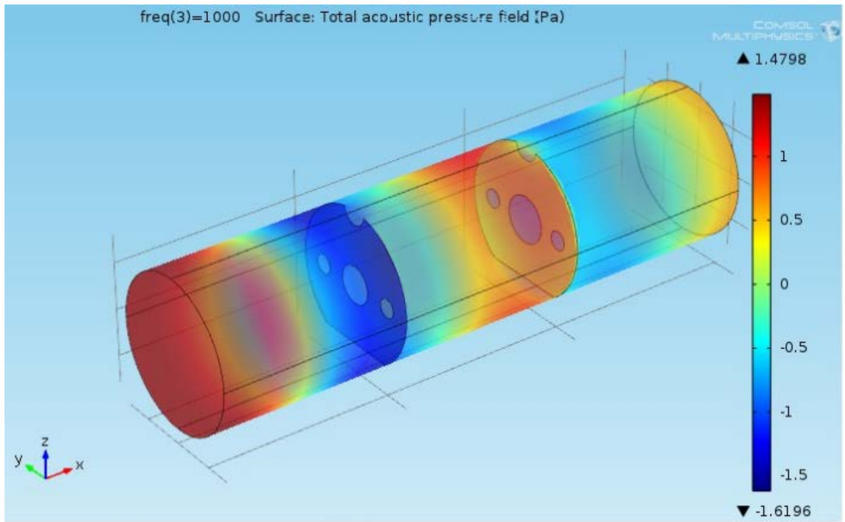
freq(3)=1000 Surface: Total acoustic pressure field (Pa)
▲ 1.4798
1
0.5
0
-0.5
-1
-1.5
▼ -1.6196
y
z
x

(a)

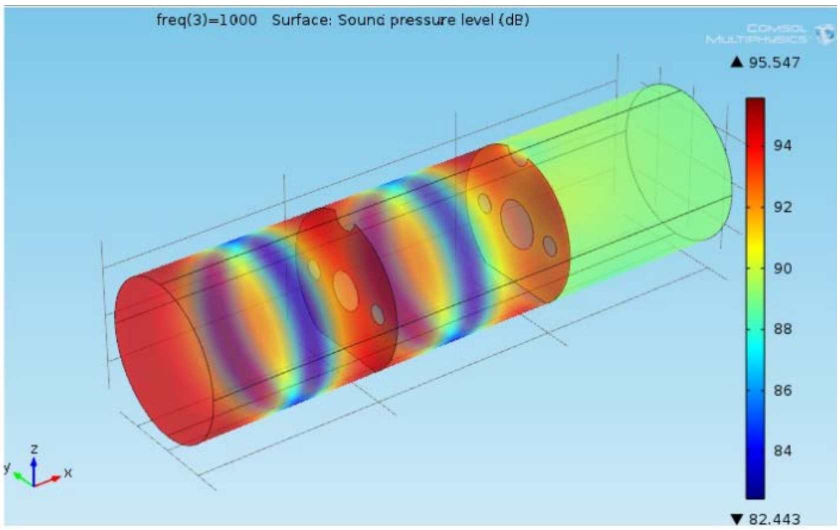
freq(3)=1000 Surface: Sound pressure level (dB)
▲ 95.547
94
92
90
88
86
84
▼ 82.443
y
z
x

(b)

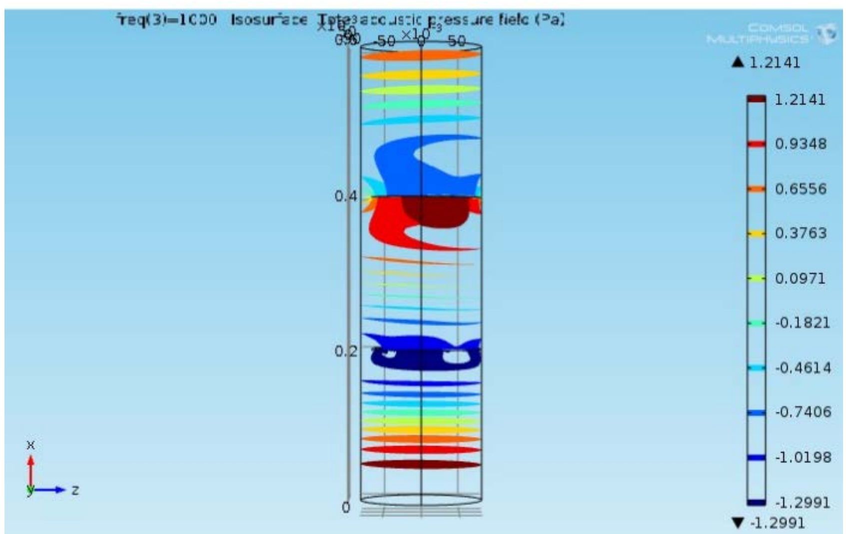
▲ 1.2141
1.2141
0.9348
0.6556
0.3763
0.0971
-0.1821
-0.4614
-0.7406
-1.0198
-1.2991
▼ -1.2991
0.4
0.2
0
x
z

(c)

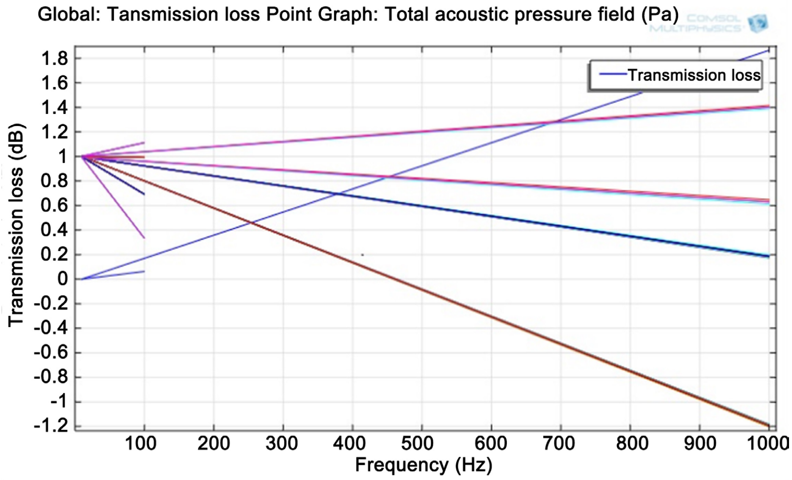

(d)

Figure 12. Conventional Baffle with one center hole and two side hole in a cylindrical tank: (a) Acoustic pressure field, (b) Surface sound pressure, (c) Iso-surface pressure, (d) Transmission loss and point graph of total acoustic pressure.

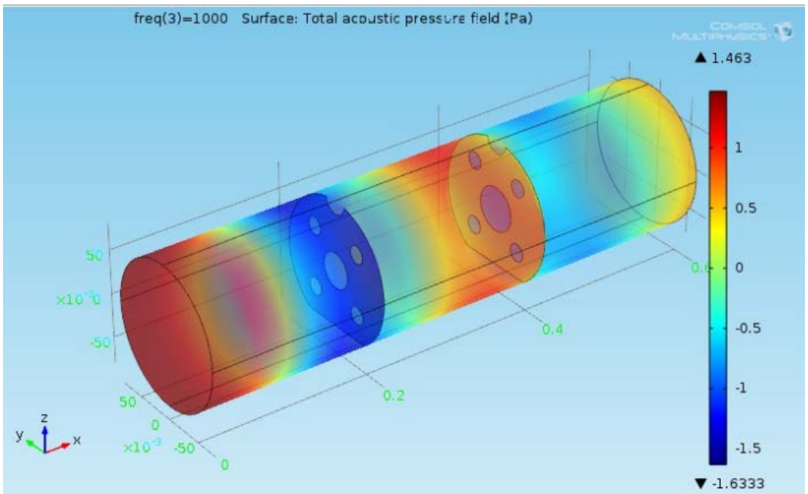

(a)

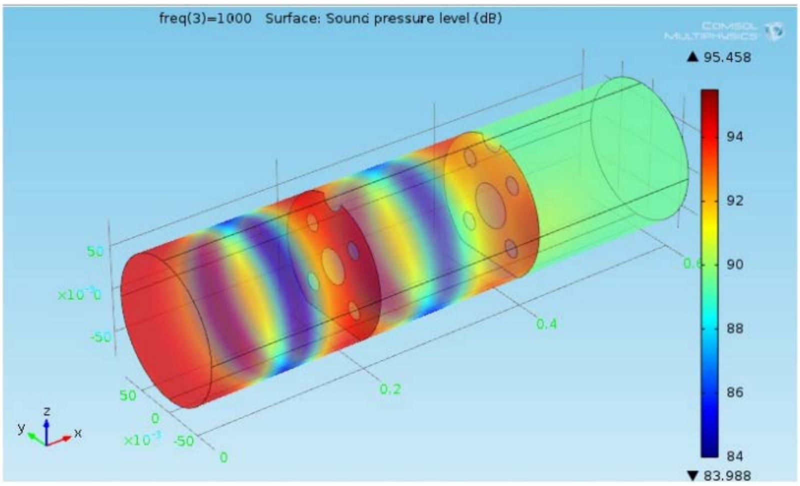

(b)

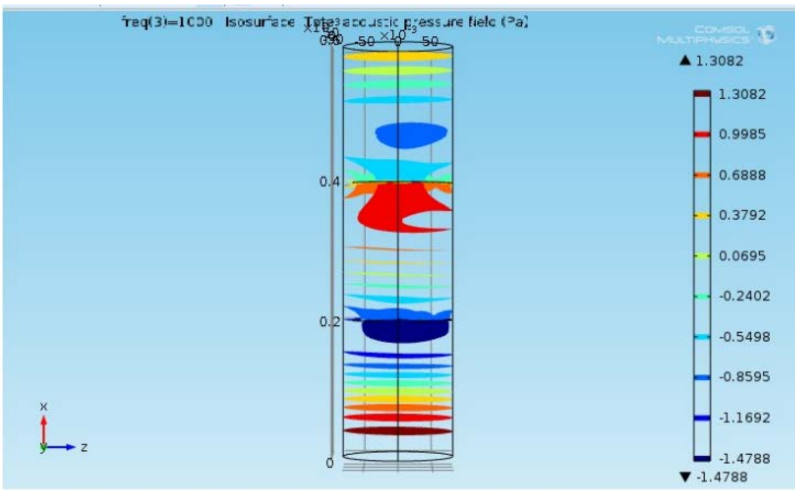

(c)

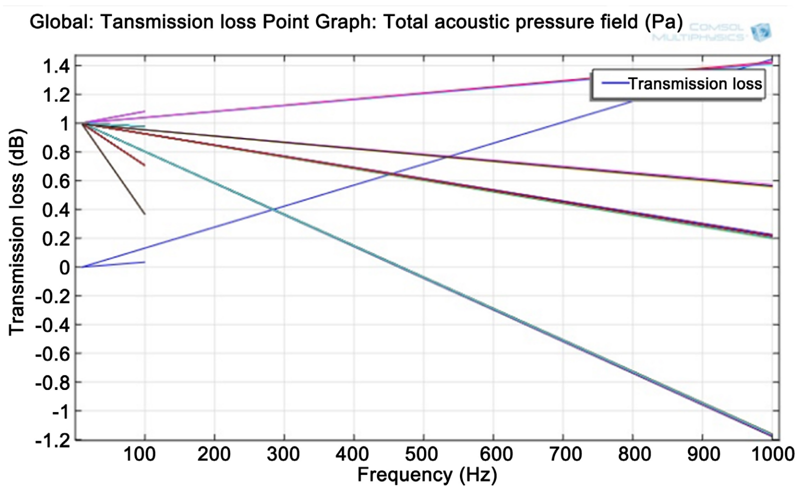

(d)

Figure 13. Conventional Baffle with one center hole (manhole) and four side holes in a cylindrical tank: (a) Acoustic pressure field, (b) Surface sound pressure, (c) Iso-surface pressure, (d) Transmission loss and point graph of total acoustic pressure.

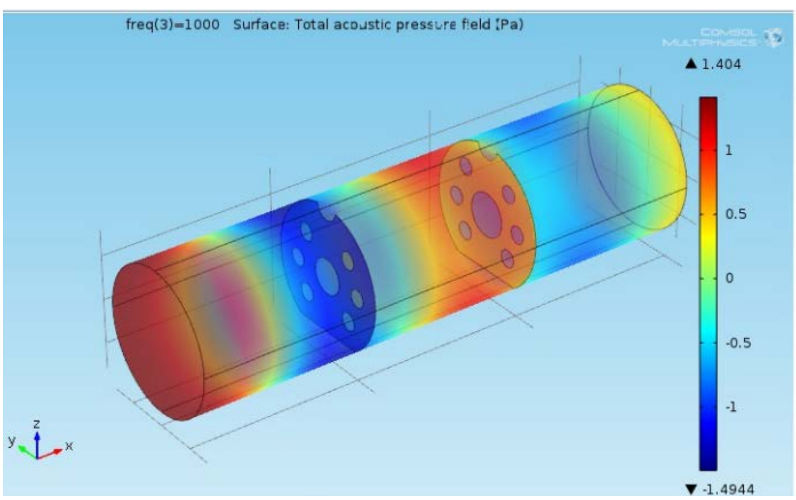

(a)

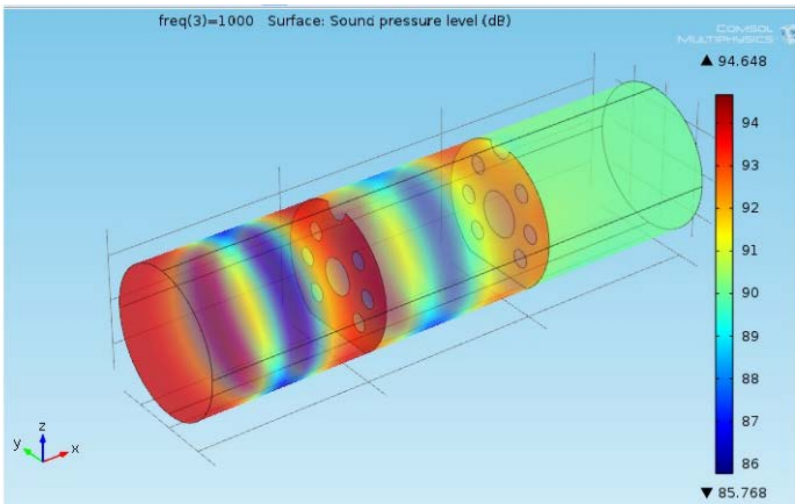

(b)

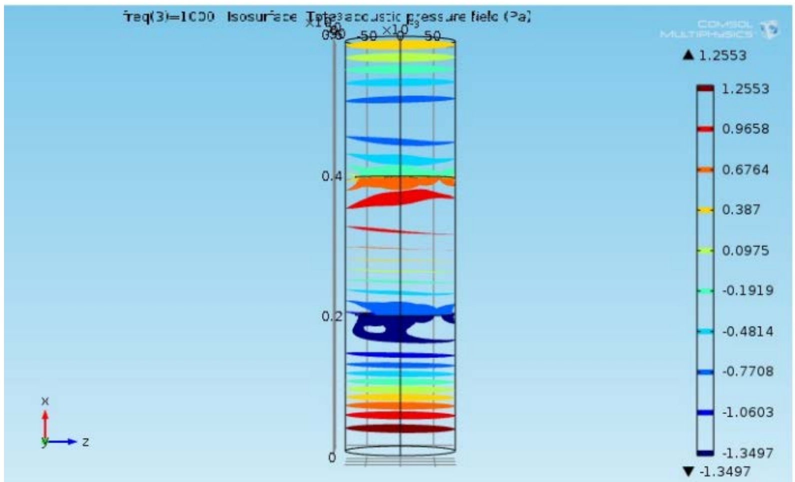

(c)

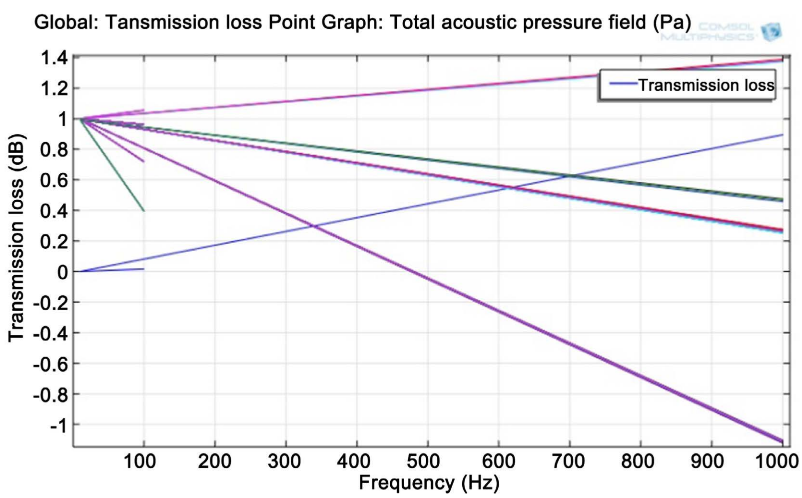

(d)

Figure 14. Conventional Baffle with one center hole (manhole) and six side holes in a cylindrical tank: (a) Acoustic pressure field, (b) Surface sound pressure, (c) Iso-surface Pressure, (d) Transmission loss and point graph of total acoustic pressure.

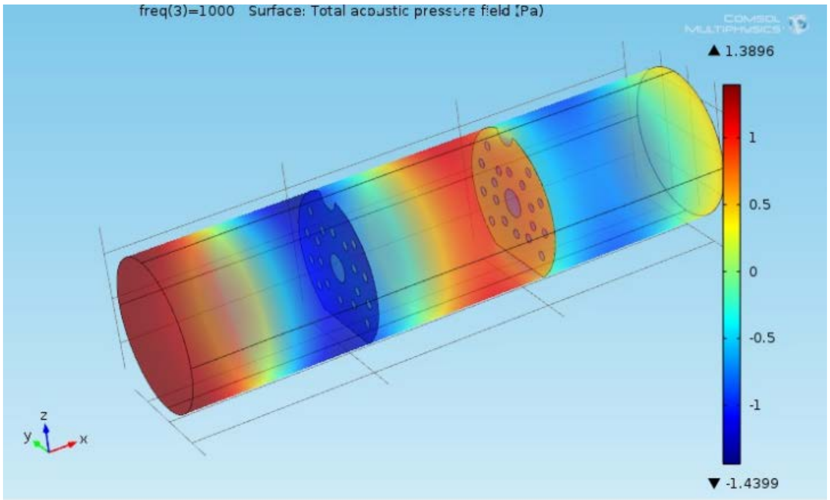
freq(3)=1000 Surface: Total acoustic pressure field (Pa)
▲ 1.3896
1
0.5
0
-0.5
-1
▼ -1.4399

(a)

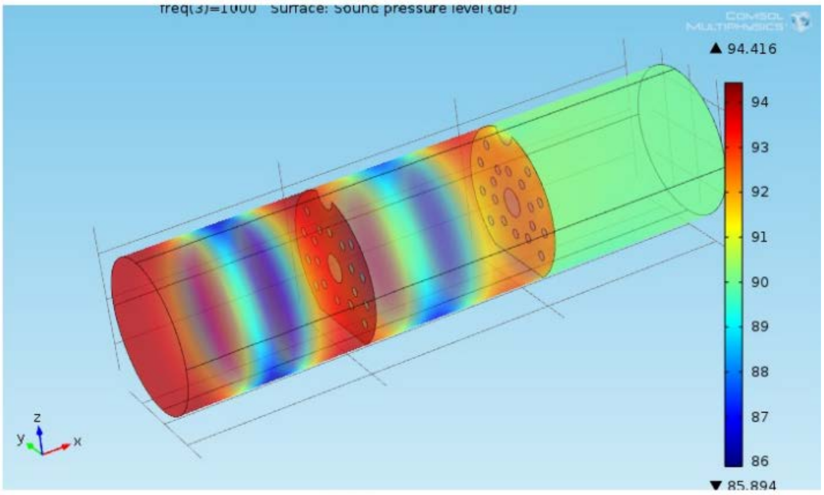
▲ 94.416
94
93
92
91
90
89
88
87
86

(b)

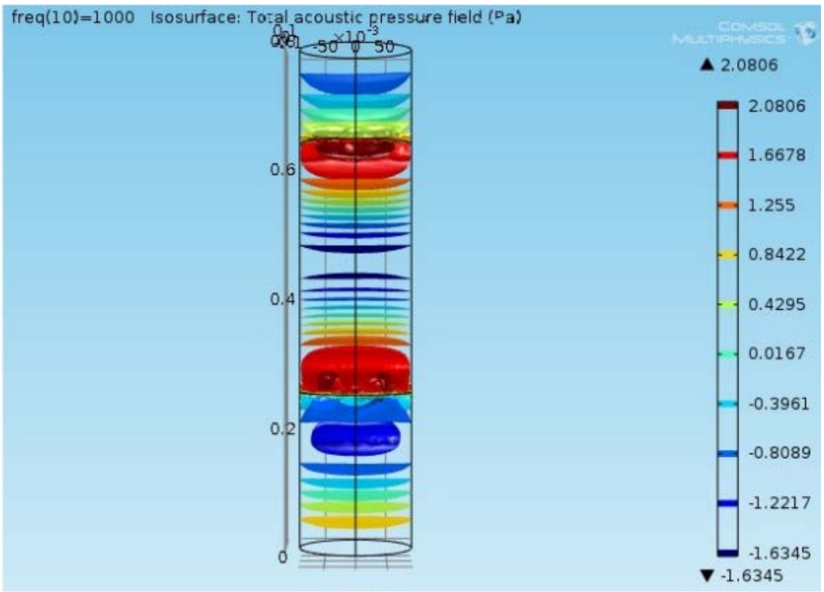
freq(10)=1000 Isosurface: Total acoustic pressure field (Pa)
0.6
0.4
0.2
0
▲ 2.0806
2.0806
1.6678
1.255
0.8422
0.4295
0.0167
-0.3961
-0.8089
-1.2217
-1.6345
▼ -1.6345

(c)

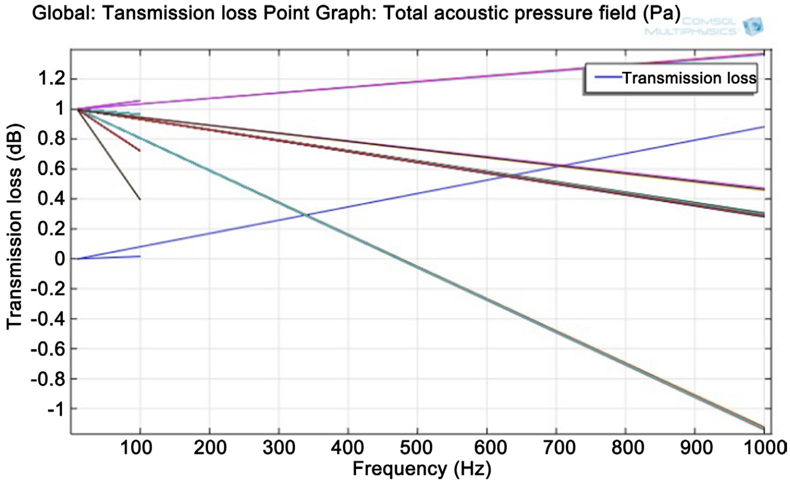

(d)

Figure 15. Conventional Baffle with one center hole (manhole) and 18 side holes in a cylindrical Tank: (a) Acoustic pressure field, (b) Surface sound pressure, (c) Iso-surface pressure, (d) Transmission loss and point graph of total acoustic pressure.

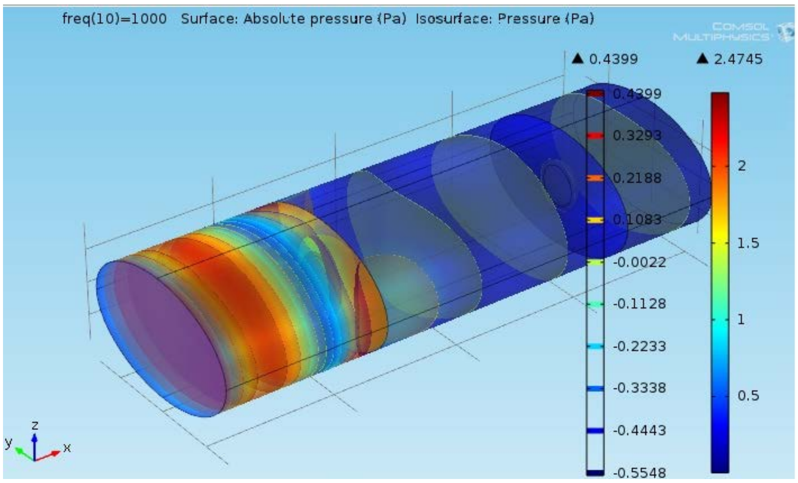

(a)

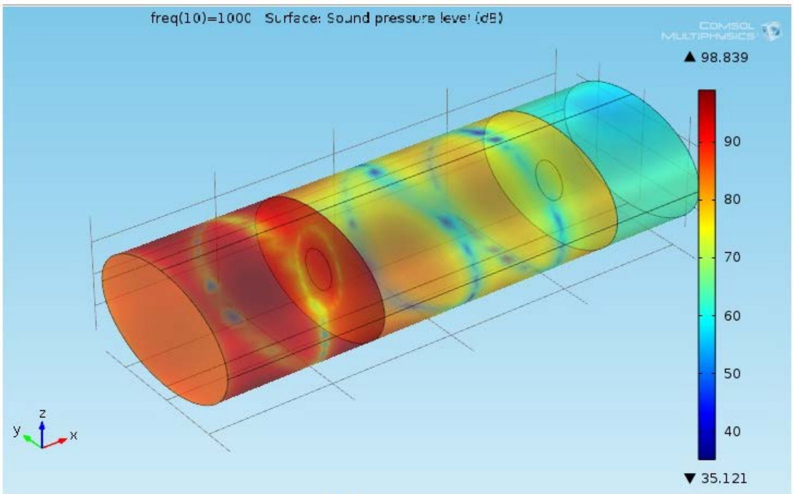

(b)

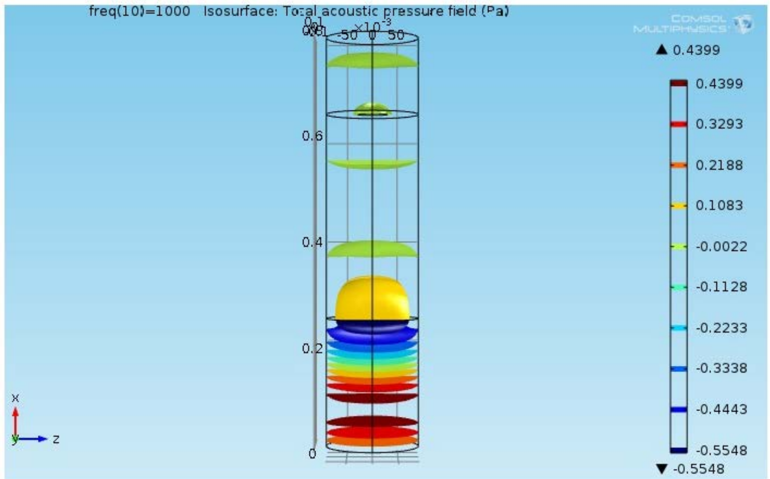

(c)

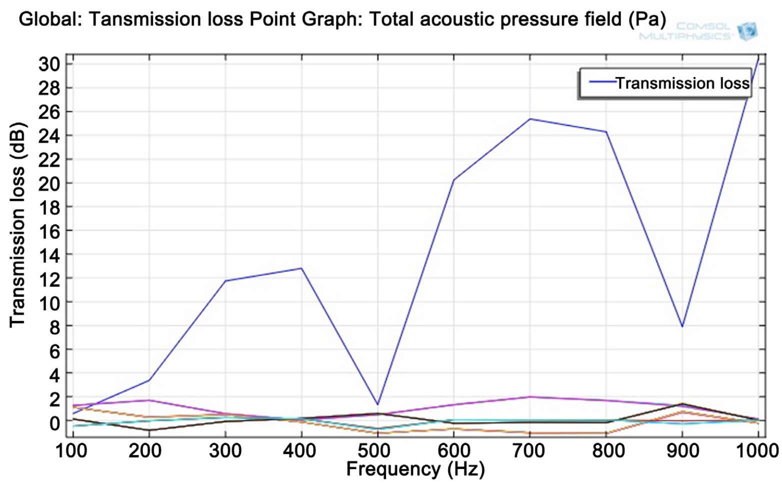

(d)

Figure 16. Conventional Baffle in an elliptical tank: (a) Acoustic pressure field, (b) Surface sound pressure, (c) Iso-surface pressure, (d) Transmission loss and point graph of total acoustic pressure.

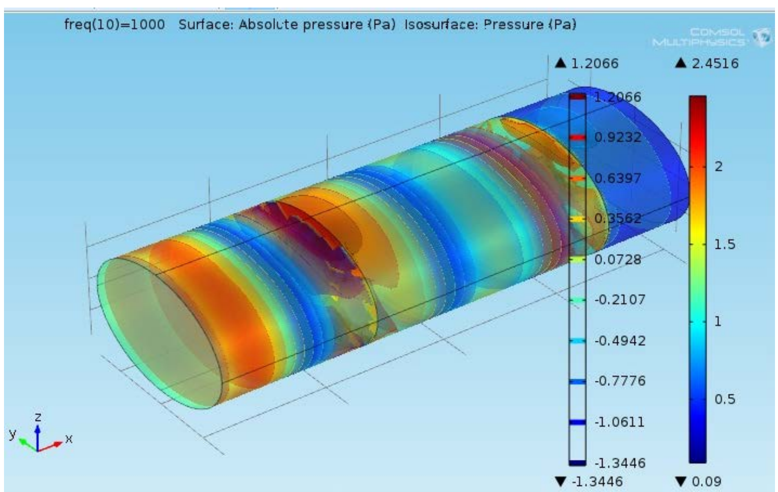

(a)

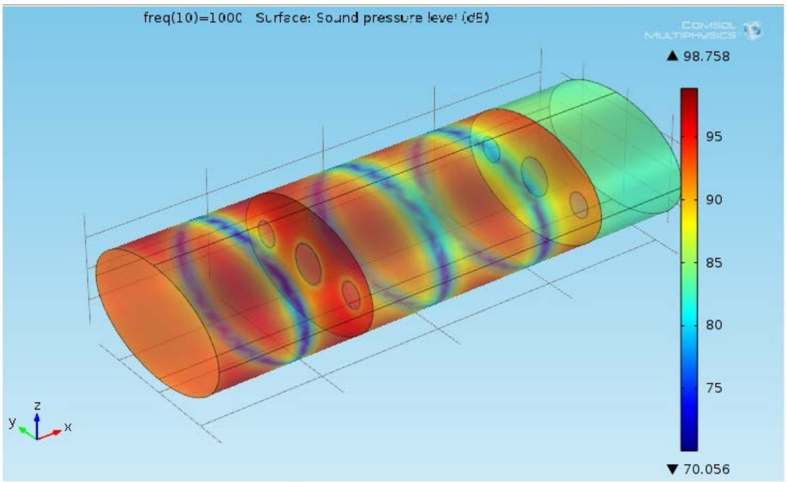

(b)

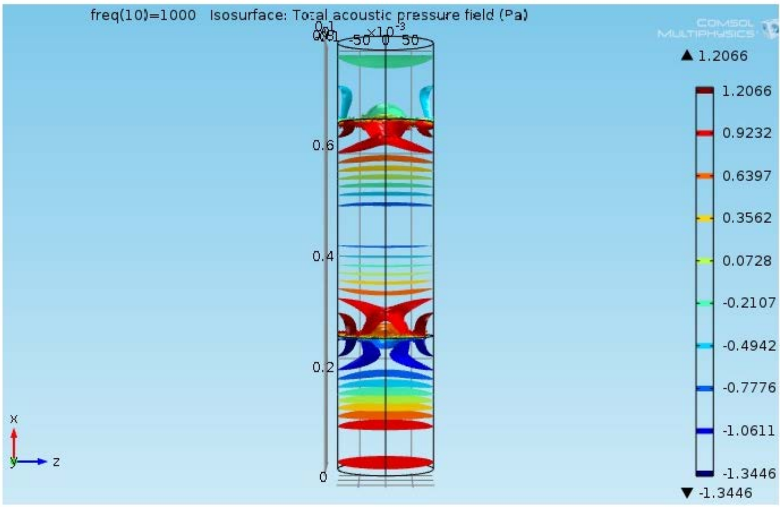

(c)

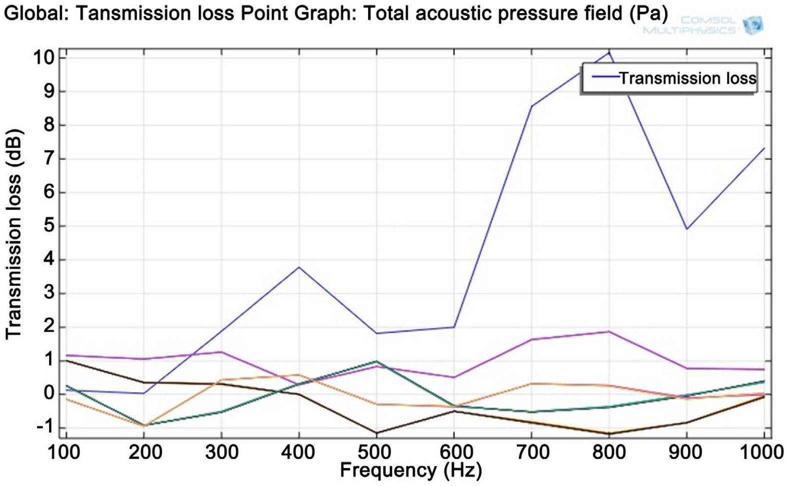

(d)

Figure 17. Conventional Baffle with one manhole and two side holes in an elliptical tank: (a) Acoustic pressure field, (b) Surface sound Pressure, (c) Iso-surface pressure, (d) Transmission loss and point graph of total acoustic pressure.

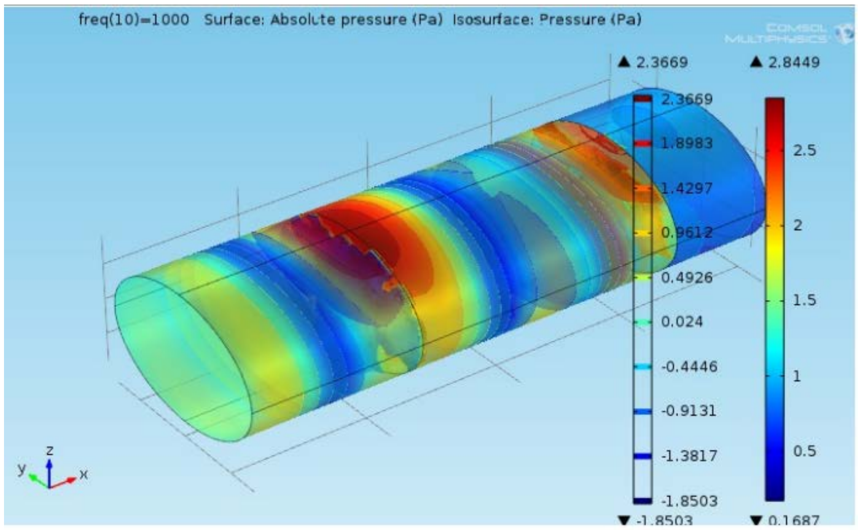
freq(10)=1000 Surface: Absolute pressure (Pa) Isosurface: Pressure (Pa)
▲ 2.3669
▲ 2.8449
2.3669
1.8983
1.4297
0.9612
0.4926
0.024
-0.4446
-0.9131
-1.3817
-1.8503
▼ -1.8503
2.5
2
1.5
1
0.5
▼ 0.1687
z
y
x

(a)

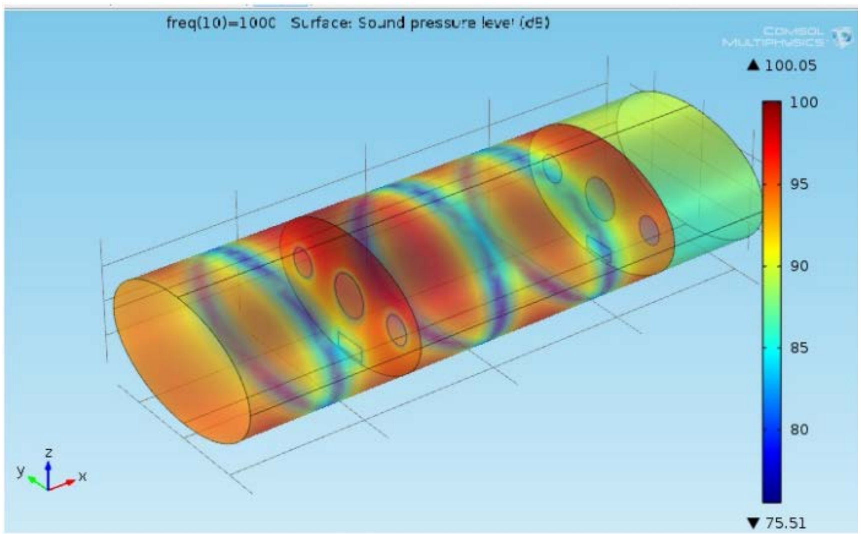
▲ 100.05
100
95
90
85
80
▼ 75.51
z
y
x

(b)

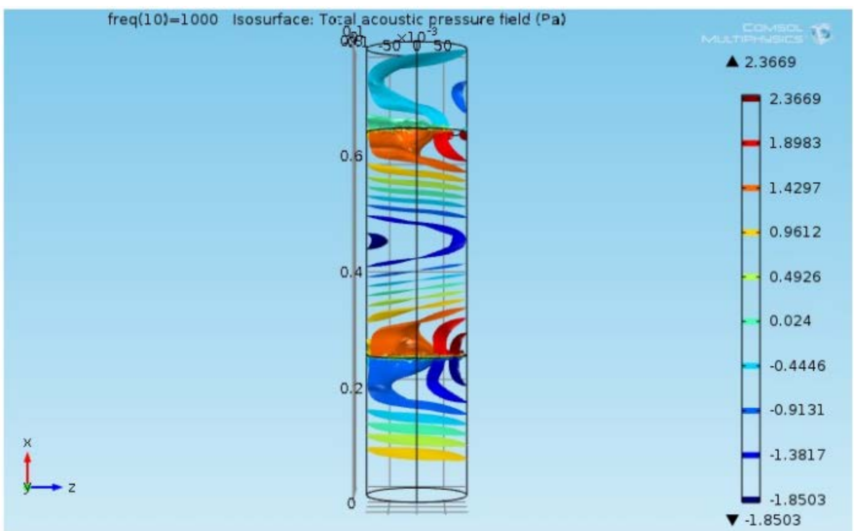
freq(10)=1000 Isosurface: Total acoustic pressure field (Pa)
0.6
0.4
0.2
0
▲ 2.3669
2.3669
1.8983
1.4297
0.9612
0.4926
0.024
-0.4446
-0.9131
-1.3817
-1.8503
▼ -1.8503
x
z

(c)

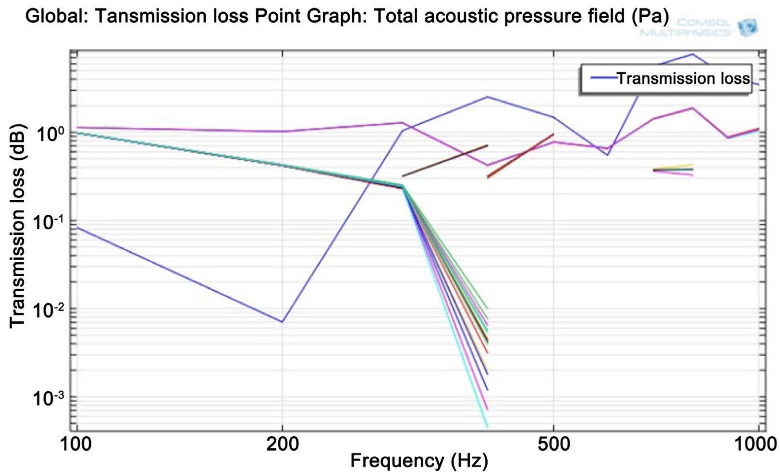

(d)

Figure 18. Conventional Baffle with one manhole, two side holes and one rectangular hole in an elliptical tank: (a) Acoustic pressure field, (b) Surface sound pressure, (c) Iso-surface pressure, (d) Transmission loss and point graph of total acoustic pressure.

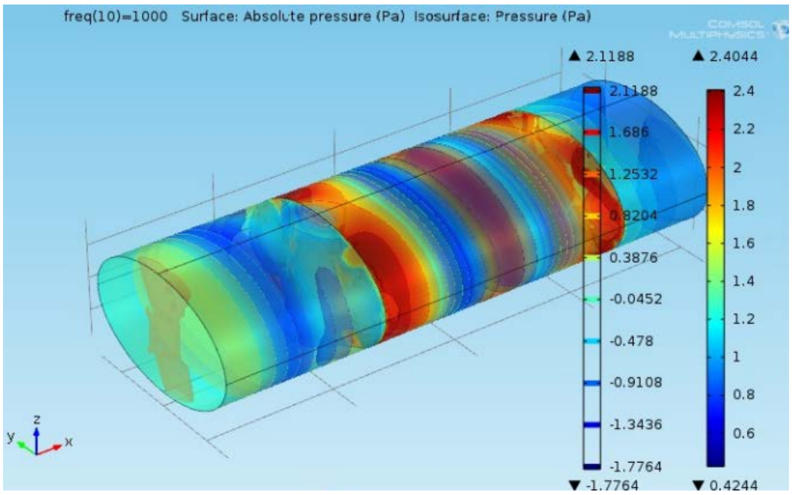

(a)

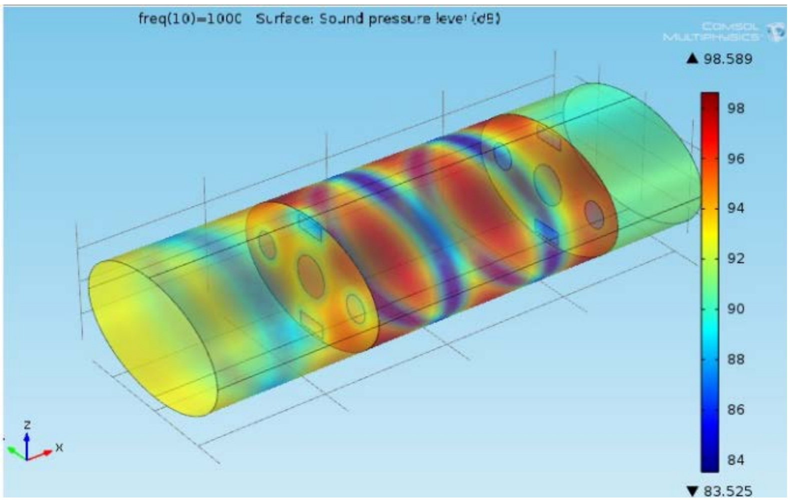

(b)

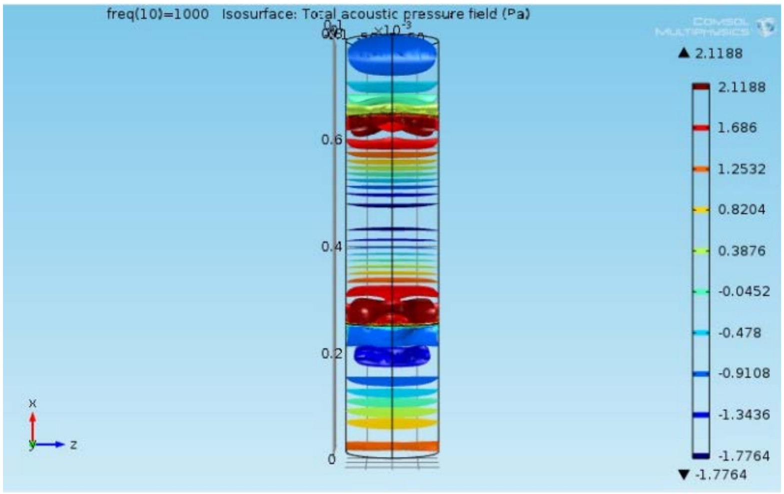

(c)

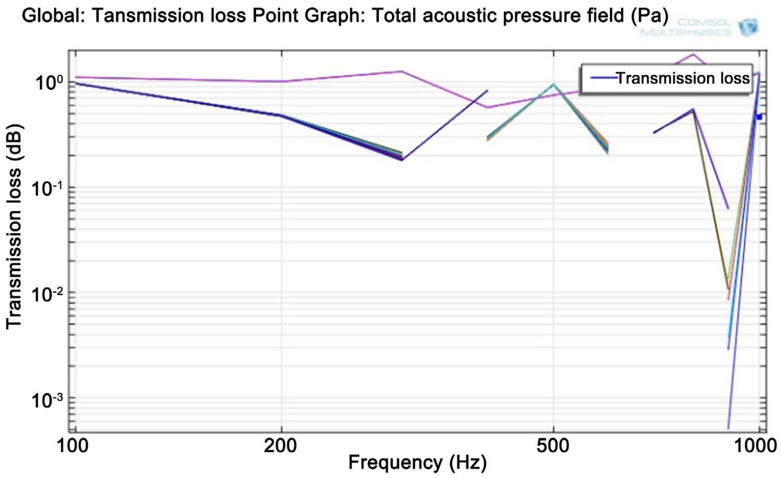

(d)

Figure 19. Conventional Baffle with a manhole and two rectangular holes in an elliptical tank: (a) Acoustic pressure field, (b) Surface sound pressure, (c) Iso-surface pressure, (d) Transmission loss and point graph of total acoustic pressure.

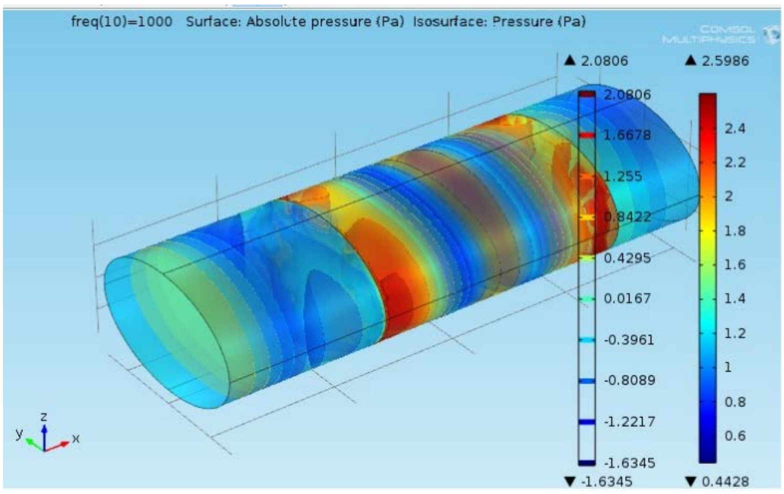

(a)

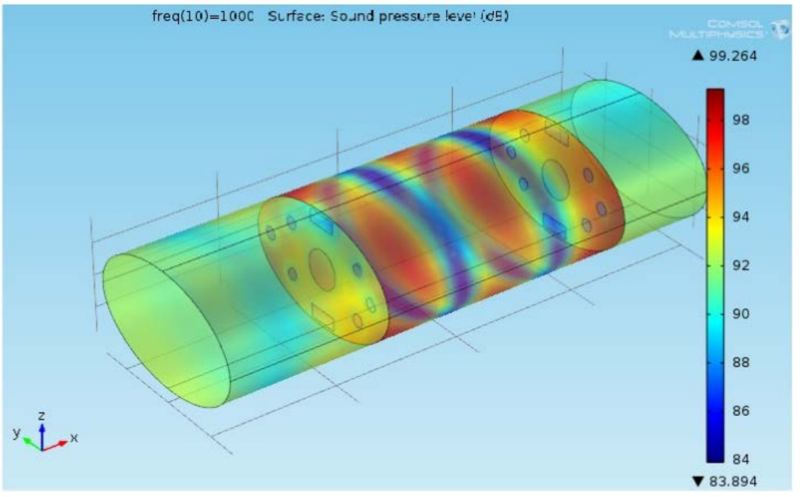

(b)

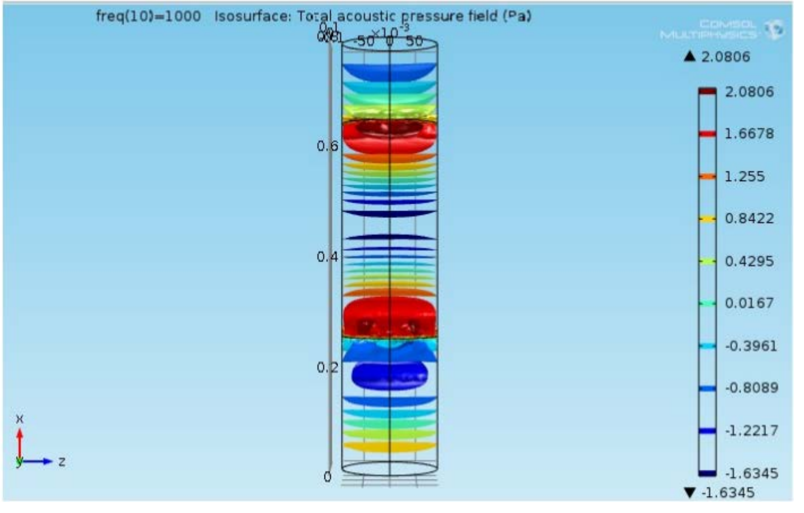

(c)

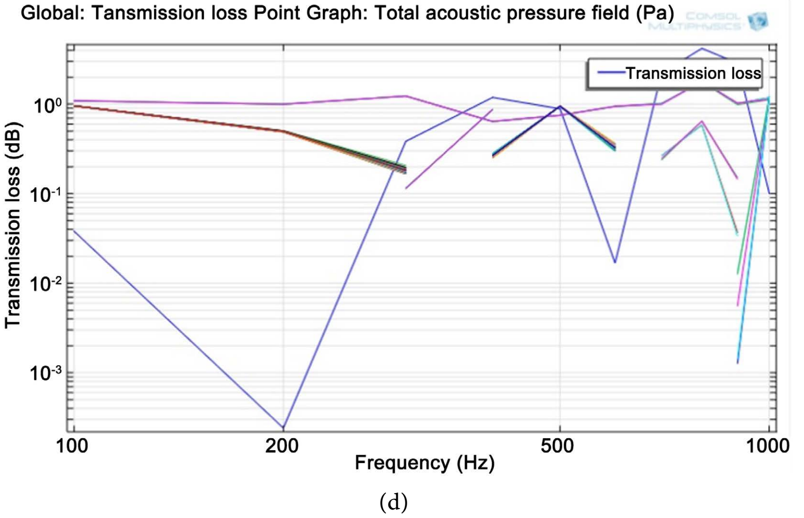

(d)

Figure 20. Conventional Baffle a man holes, six side holes and two rectangular holes in an elliptical tank: (a) Acoustic pressure field, (b) Surface sound pressure, (c) Iso-surface pressure, (d) Transmission loss and point graph of total acoustic pressure.

For the cylindrical storage tank, the Baffle with average perforations (4 to 7 holes with respect percentage of material off-cutting recommended in **Figure 7**) shows more damping responds as seen in **Figure 10(c)**, **Figure 13(c)** & **Figure 15(c)** were the blue color around the first Baffle surface is without bubbles reflecting a smooth slushing possibility via the Baffle. Typical values in these blue zones vary between −1.4607 Pa to −0.849 Pa, −1.4788 Pa to −0.8595 Pa and −1.298 Pa to −0.7326 Pa respectively. But due to multiple perforations of the Baffle in **Figure 15**, the overall strength of the tank is affected and thus fairly recommended. On the other hand, the elliptical tank also portrayed a better damping response for Baffles having 5 perforated holes as seen in **Figure 19(c)** where the is a uniform sloshing shown by the blue color around the first Baffle surface with typical values in this blue zone varying between −1.3436 Pa to −0.9108 Pa.

4.2. Experimental Method

4.2.1. Focus

Mindful of the fact that for every sloshing environment, there is a force exerted on the surface of the Baffle, the aim of this area of study is to experimentally determine the magnitude of sloshing on different Baffle configurations through the measurement of FLUID LOST ability for a given Baffle. Obviously, from a layman's point of view, if the Baffle is simply made without any hole and placed in a test tunnel or tank where fluid is made to pass, the flow will be blocked completely then they will be no Lost of fluid. But if there is a broken-out section or hole on the Baffle and placed in the same test tank then during functionality, fluid will pass through the hole, hence there will be losses and depending on the type of baffle design the fluid lost will vary. In this line of thoughts the fluid flow ability equated to be sloshing effects can be measured.

4.2.2. General Tank Specifications

The specifications here are for the Storage tanks of inflammable and non-flammable, materials that are harmful to the environment when out of control. The material should have a density of 1.1 kg/dm^3 for EN 12285 class A and up to 1.9 kg/dm^3 for tanks EN 12285 class B and DIN6616. This extract of information serves as a guide to the realization of a usable storage tank. Other technical specifications include:

- Design according to EN 12285-2 class A or B or according to DIN6616
- Technical documentation approved by Notified Body
- Basic material – S235JR according to EN10025-1

4.2.3. Tank Characteristics (Figure 21)

- Single or multi-chamber tank
- Working pressure: max 0.5 bar
- Working temperature: from −20 degrees Celsius to + 50 degrees Celsius

4.2.4. Tightness

As mentioned earlier, all Tanks must be tested after manufacturing. The values

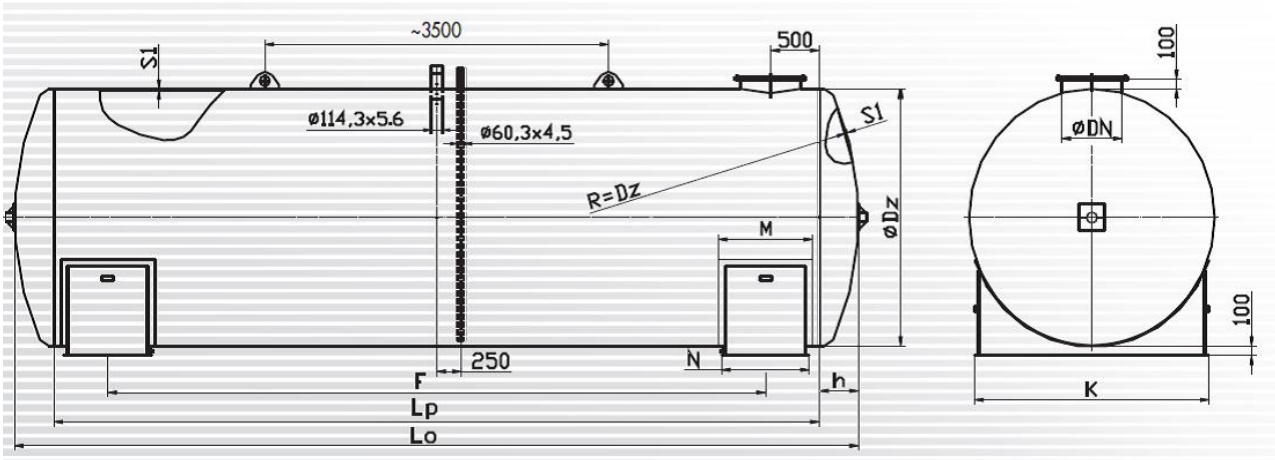

Figure 21. Tank design [16].

in **Table 2** below presents the post-manufacturing pressure test of both inner tank and inter-space according to norms.

Thus in a more summarize manner, Storage tanks applicable to this domain of study are classified with respect to their Designation, classes and working pressures. The table below (**Table 3**) shows some values commonly used nowadays.

4.2.5. Outer Surface

Abrasive grit-blasted to grade Sa 2.5 according to PN-ISO 8501-1 and painted in C3 standard or higher.

4.2.6. Standard Equipment

Manhole DN600 with gasket Steel supports for EN-tanks: 1.9 N/mm^2 for DIN 6616-tanks 0.15 N/mm^2 transport grips ladder, platform, railing Filling pipe, suction pipe, venting pipe

4.2.7. Optional Equipment

- Overfill valve, venting valve, de-watering pipe
- System and control pipes
- Contents measuring

With the help of a prototype experimental tank with a reduction in scale of up to 0.01 and taking into consideration the corresponding equality of dimensions used the various Baffles used in the computerized studies seen in the chapter above, the evaluation of the sloshing phenomenon in the presence of different Baffles has been reached. The figure below is a representation of the Experimental setup.

The design involves two particular components to facilitate the outcome of the experiment. The first is the prototype tank opened on both ends, having a sit for the baffles to be mounted and a close to frictionless sliding mechanism to facilitate the free longitudinal displacement of the Baffle along the tank. **Figure 22** below shows the design setup.

This mechanism also carries the pulley to relay the slightest displacement of

Table 2. Tank nomenclature.

Measures & weight [ca]																	
Values	Diameters	Length	Manhole	Weights		Supports						Well thickness				Lifting hugs	Strength ring
				Class A	Class B	Class A			Class B			Class A		Class B			
V	Or	Lo	DN	G	G	F	N	K	F	N	K	S1	S2	S1	S2		T80
[m²]	[mm]	[mm]	[mm]	[kg]	[kg]	[mm]	[mm]	[mm]	[mm]	[mm]	[mm]	[mm]	[mm]	[mm]	[mm]	[pcs]	[pcs]
3	1600	2040		946	1020	700			950							2	-
5	1600	3040		1266	1340	1700			1950							2	-
7	1600	3840	600	1518	1590	2500	150	1600	2750	350						2	-
10	1600	5540		2051	2126	4200			4450							2	-
13	1600	7040		2513	2592	5700			5950							2	-
16	1600	8540		2992	3069	7200			7450			5	3	5	3	2	1
10	2000	3660		2143	2335	2000			2200							2	1
13	2000	4660		2588	2780	3000			3200							2	-
16	2000	5660		3044	3237	4000			4200							2	-
20	2000	6810	600	3567	3761	5150	200	2000	5350	600						2	-
25	2000	8660		4394	4588	7000			7200							2	-
30	2000	10,160		5133	5328	8500			8700							2	1
36	2000	11,960		5943	6138	10,300			10,500			6	3	6	3	2	1
20	2500	4800		3838	4653	2750			2850							2	-
25	2500	5800		4456	5335	3750			3850							2	-
30	2500	6800		5068	6010	4750			4850							2	1
40	2500	8800	600	6373	7442	6750	250	2500	6850	950						2	1
50	2500	10,800		7599	8796	8750			8850							2	1
60	2500	12,800		8915	10,239	10,750			10,850							2	2
70	2500	14,800		10,136	11,586	12,750			12,850			6	4/5	7	4/5	2	2
40	2900	6900		6722	9016	4550			4450							2	1
50	2900	8400		7990	10,504	6050			5950							2	1
60	2900	9900	600	9175	11,909	7550	300	2900	7450	1350						2	1
70	2900	11,400		10,347	13,301	9050			8950							4	2
80	2900	12,900		11,612	14,786	10,550			10,450							4	2
100	2900	15,900		13,974	17,588	13,550			13,450			7	4/5	9	4/5	4	2

Table 3. Tank designation, classes and working pressures.

Designation	Class	Working Pressure
EN 12285-2	Class A	0.3 bar/0.4 bar
EN 12285-2	Class B	2.0 bar/0.6 bar
DIN 6618	-	2.0 bar/0.6 bar

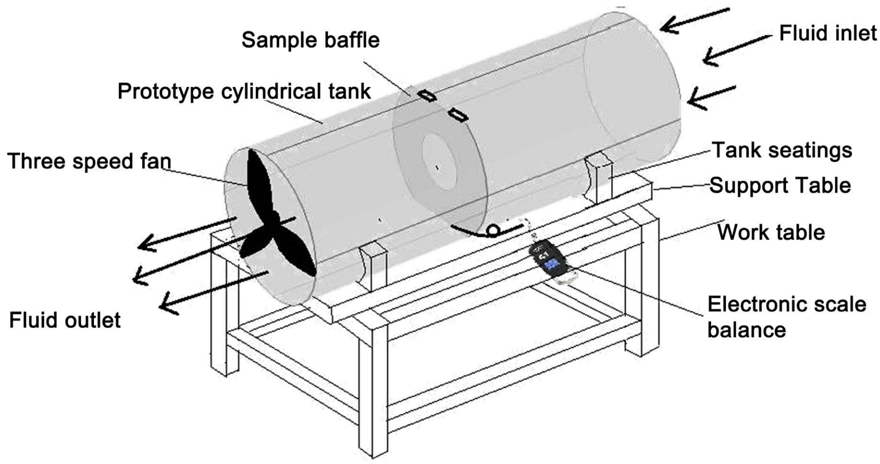

Figure 22. Design of the experimental setup.

the baffle to a lever articulated at the middle and the other extreme acts on the measuring scale. The second is 230 V a.c ROYAL Fan with speed one set at 600 rpm, speed reaching 1200 rpm and speed at 1800 rpm all at 60 Hz.

NB: For this experiment and for the purpose of accuracy, only speed two and three were used. This is because according to the graph of the fan's torque characteristics as seen below, while at the first speed, the response was not optimal to be considered (**Figure 23**)

4.2.8. Operation

Generally, the test Baffles samples are of thickness 0.08 mm with an external major diameter of 20.5 mm. Any other section removed from each baffle is in percentage with respect to the total surface area. The functionality of the system is in correspondence to the pictorial view of the final setup as seen below in **Figure 24**. A little toast was given to the air canalization by providing a conical casing linking the fan diameter and the inlet diameter of the test tank. This is so because the diameter of the fan blade cage in real life is larger than that of the test tank.

During operation, the following step are taken:

1) The baffle is mounted on its sitting while tht making sure it does not touch the walls of the test tank.

2) Carefully verify and adjust the tension of the twin on the pulley.

3) Put on the fan at speed 2 and wait for 10 seconds for it to reach its maximum allowable rotation, then record the corresponding weight exerted on the scale and switch to speed three to record the corresponding weight too.

4) Switch on the fan and repeat the process for every baffle design.

The following cylindrical and elliptical samples presented in **Figure 25** were produced and evaluated.

4.2.9. Result and Discussion of the Experiment

The measurement of the resistance to fluid flow per baffle design is equated at LOSS. Knowing that the purpose of a Baffle in a tank is to dampen sloshing. There

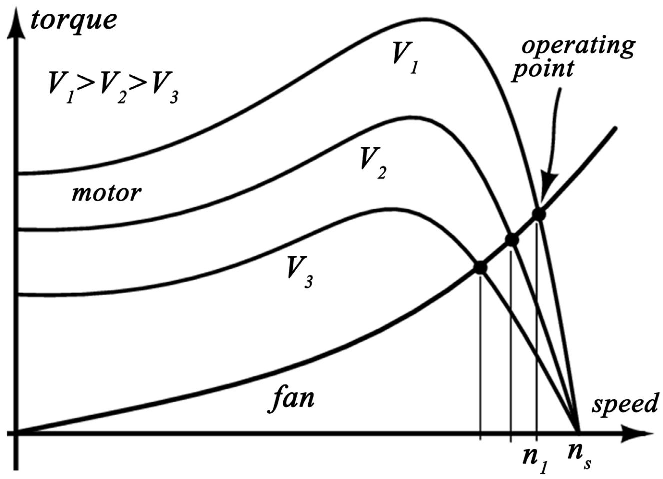

Figure 23. Graph of torque variation with respect to the speed of a Royal fan [18].

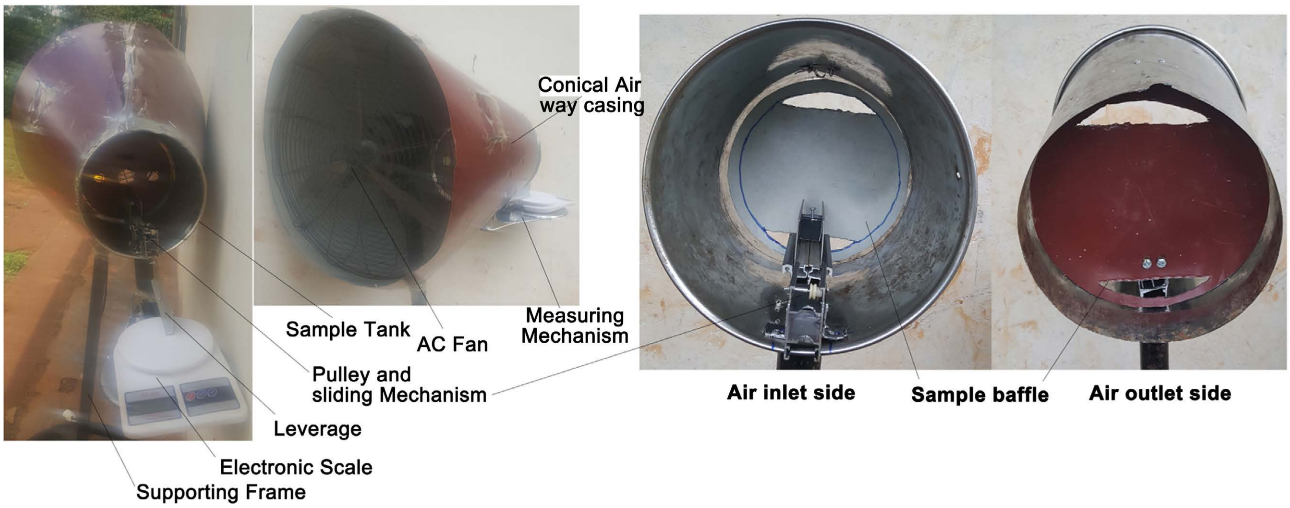

Figure 24. Image of the experimental setup.

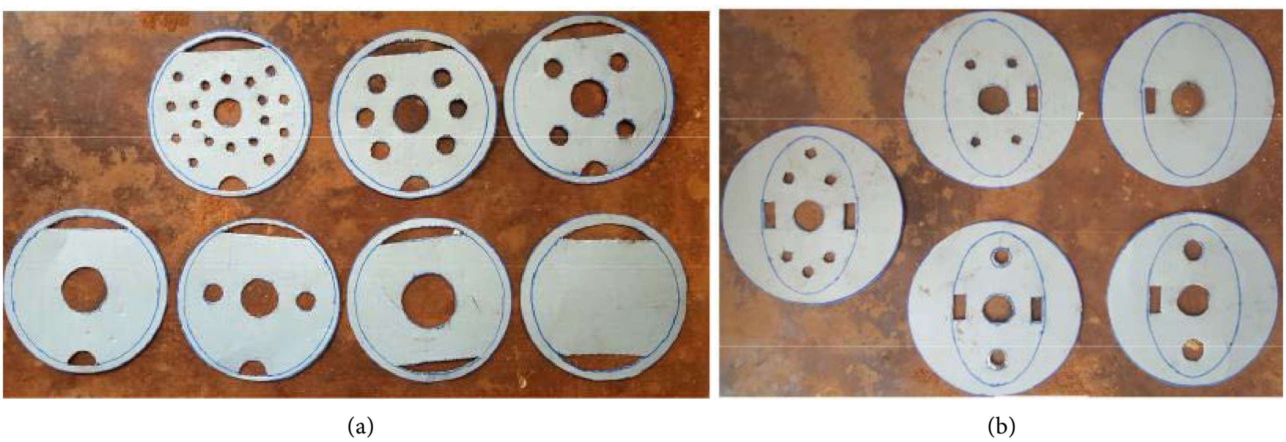

Figure 25. (a) Cylindrical tank Baffle test pieces, (b) Elliptical tank Baffle test pieces.

is therefore an ideal baffle design to provide an optimal sloshing response such that it is not too much nor too little. In this elaboration, a sample baffle that has a greater measurement value for LOSS in terms of grams on the scale indicates or means that it acts more like a resistance thus dampening ability is high and when

A- Cylindrical Tank data sheet				
Design	**Number of holes**	**Applied at 1200rpm in Grams**	**Applied weight at 1800 rpm in Grams**	**Average weight in Grams**
	2	55	80	67.5
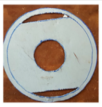	3	57	75	67
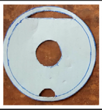	3	60	75	67.6
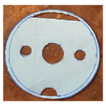	5	64	59	61.5
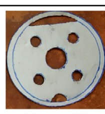	7	46	66	57.5
	9	46	48	47
	21	70	75	72.5
B- Elliptical Tank data sheet				
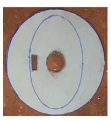	2	45	56	50.5
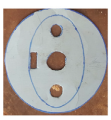	4	40	47	87
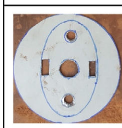	4	63	69	66
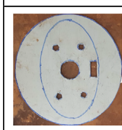	6	45	50	47.5
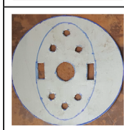	9	73	89	81

Figure 26. Data was collected for cylindrical and elliptical experiments.

applicable in the industry the fluid sloshing action will create a high reaction and it is dangerous particularly during Braking.

Conversely, if the sample baffle that has a lesser measurement value in grams on the scale it shows that it has less resistance thus its dampening ability is too low and when put into use, the sloshing action will not be felt leading to unwanted thrust on the baffles or the entire tank walls and still dangerous. The resulting graphs (Figures 26-30) for the various test conducted are as seen below.

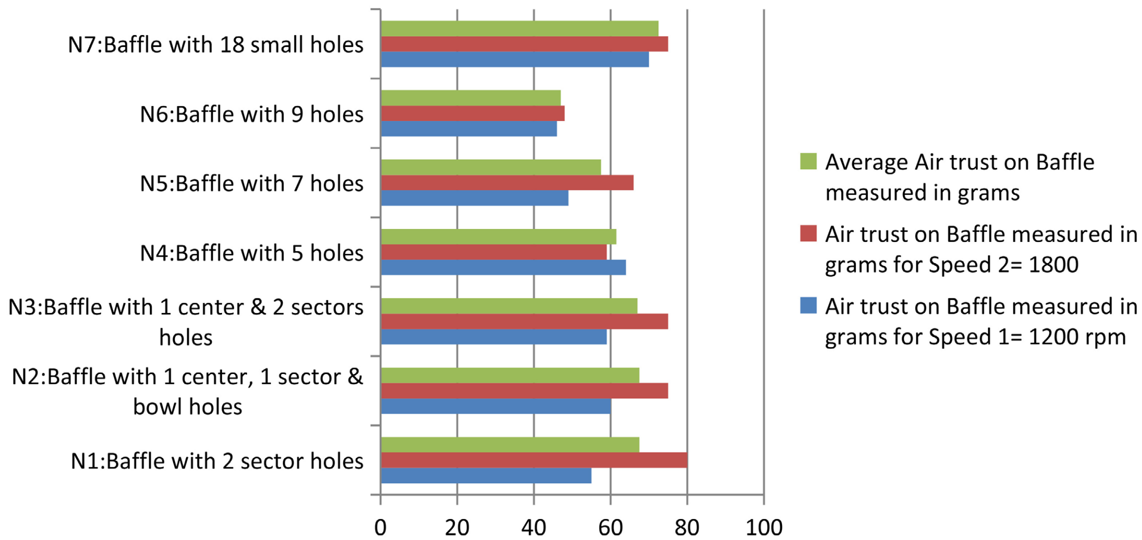

Figure 27. Bar chart of cylindrical tank baffle test piece.

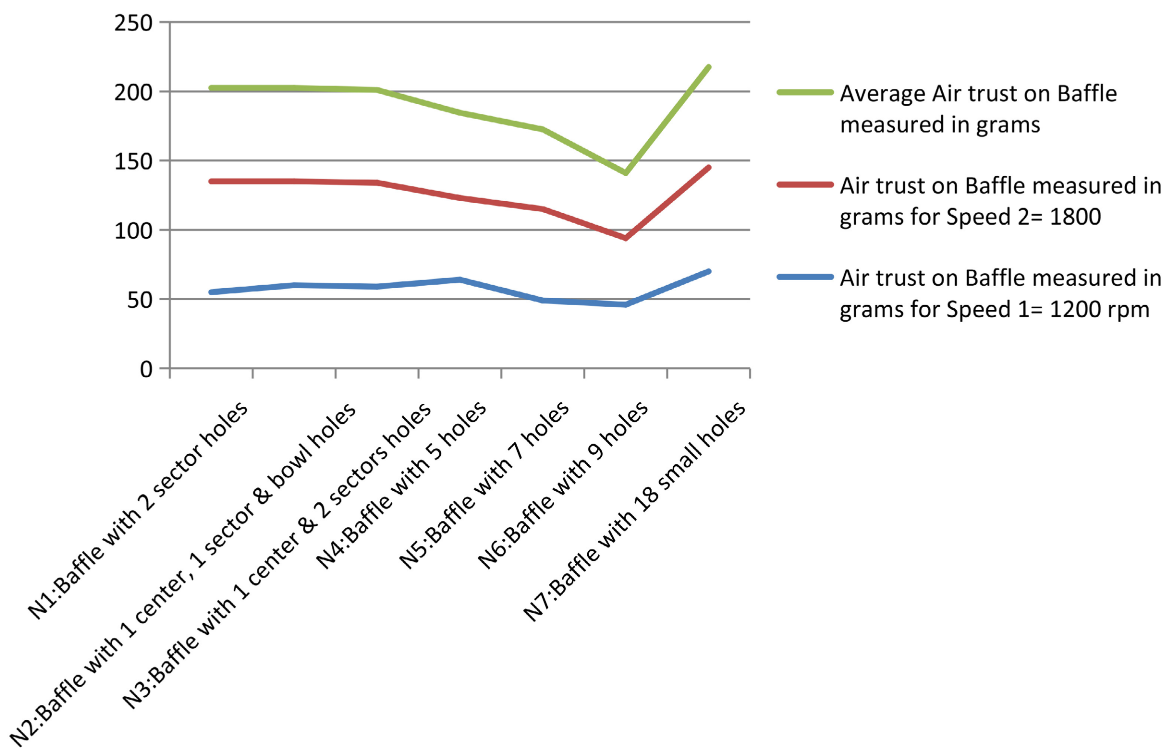

Figure 28. Graph of cylindrical tank baffle Test pieces.

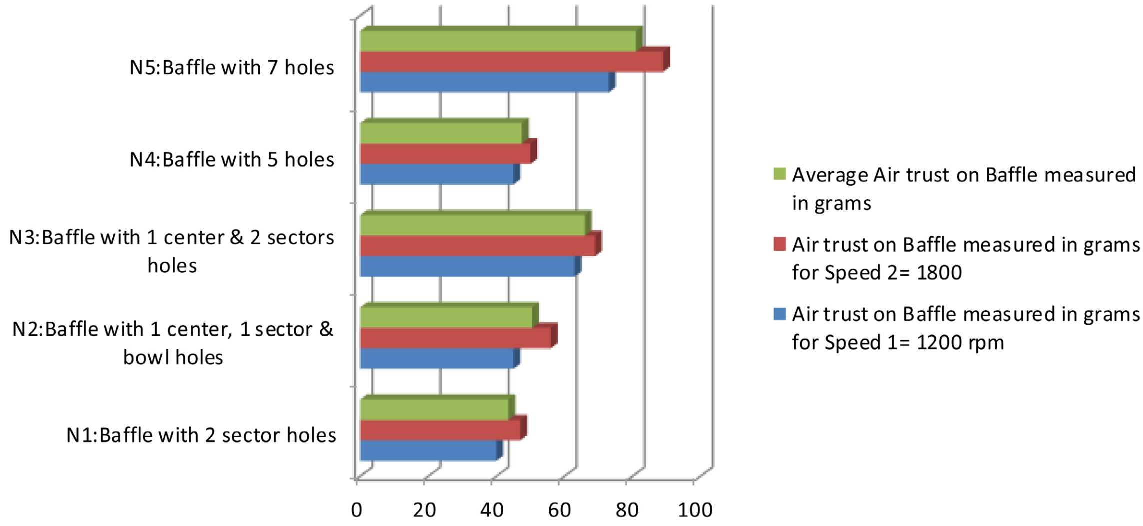

Figure 29. Bar chart of elliptical tank baffle test pieces.

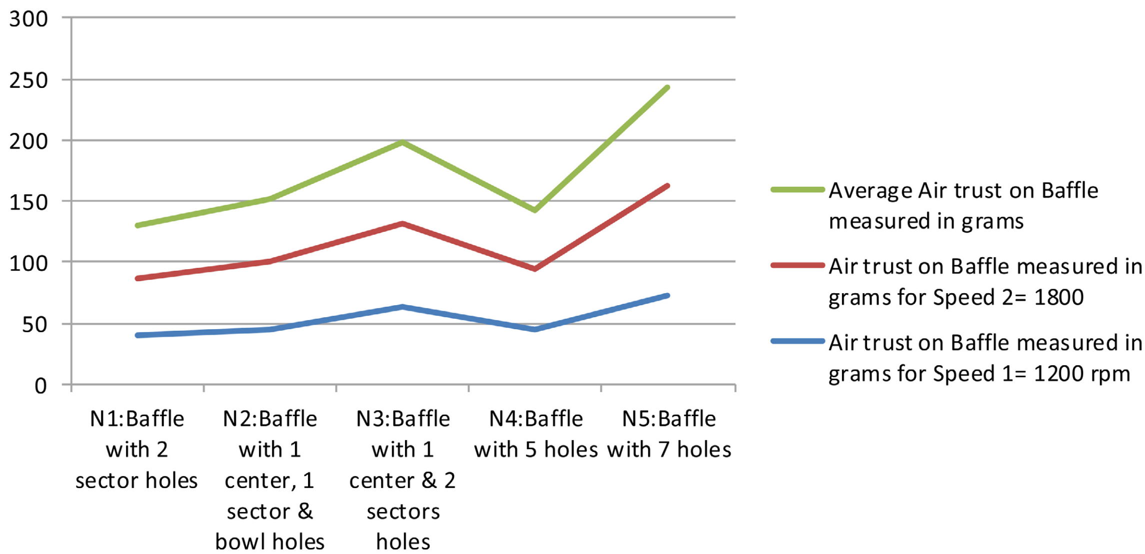

Figure 30. Graph of elliptical tank baffle test pieces.

5. Conclusion

Mindful of how dangerous petroleum material can be if poorly handled we are looking at improvement on safety during emergency braking by elaborating on the effectiveness of various Baffle designs usable in storage tanks for transporting petroleum products when it comes to damping sloshing waves. This study therefore compares computerized and experimental investigation for cylindrical and elliptical storage tanks used for transporting petroleum products by trucks. The particular attention here is on vertical placed Baffles with variety of perforated designs placed under pressure acoustic iso-surface loss for the computerized study and hydrodynamic loss of fluid during sloshing with respect to each Baffled for the experimental case study. Both are a check for the effectives of damping during approximated during emergency braking excitation where we have critical fluid sloshing. This is in line with predicting the best design construction suitable for future application. The result obtained within a safe working pressure margin shows that the conventional type with one central large hole and a small opening at the bottom does not prove to be very effective in damping sloshing; neither is the Baffle with many perforations. The designs with an average multiple holes rather than the usual face-centered are more efficient in fluid sloshing particularly during braking. The application of these designs provides a uniformly distributed damping during fluid sloshing in the tank thereby reducing the magnitude of forward thrust that can be created by the conventional Baffle type during emergency braking which sometimes sways the truck carrying the container to unwanted directions against the will of the driver and thus improving on safety.

Funding

This research received no external funding.

Acknowledgements

This research was partly Facilitated by:
- The Management of HORIZONE 7 Bonaberi Douala and
- The Ministry of transport in Partnership with the Ministry National security Yaounde - Cameroon
- The Mechanical Engineering Department of IUT Banjun

Data Availability Statement

All data used in this article are freely available.

Conflicts of Interest

The author declares no conflict of interest.

References

[1] Newsletter Maville: Récapitilatif des accidents au Cameroun of May 2023. https://www.crtv.cm/2022/05/accidents-de-la-route-des-statistiques-qui-interpellent/

[2] Cameroon tribune (Yaounde) (2012). https://www.cameroon-tribune.cm/

[3] Technical Documents 8787 (2015). https://ins-cameroun.cm/wp-content/uploads/2021/02/0CHAPITRE-12_-SECURITE.pdf

[4] Lyu, W.J., Ould, E.M., Robert, P. and Jens, N. (2017) Experimental and Numerical Investigation of Sloshing Using Different Free Surface Capturing Methods. *Applied Ocean Research*, **68**, 307-324.

[5] Papaspyrou, S., Valougeorgis1, D. and Karamanos, S.A. (2004) Sloshing Effects in Half-Full Horizontal Cylindrical Vessels Under Longitudinal Excitation. *Journal of Applied Mechanics*, **71**, 255-265.https://doi.org/10.1115/1.1668165

[6] Maleki, A. and Ziyaeifar, M. (2007) Sloshing Damping in Cylindrical Liquid Storage Tanks with Baffles. *Journal of Sound and Vibration*, **311**, 372-385.

[7] Anramson, H.N. and Garza, L.R. (1964) Some Measurement on the Effects of Ring Baffle in Cylindrical Tanks.

[8] Ebrahimiam, M., Noorrian, M.A. and Hassan, H. (2015) Free Vibration Sloshing Analysis in Axisymmetric Baffled Containers under Low-Gravity Condition. *Microgravity Science and Technology*, **27**, 97-106. https://doi.org/10.1007/s12217-015-9414-4

[9] Martellucci, L. and Giannini, M. (2021) Regenerative Braking Experimental Tests and Results for Formula Student Car. *Journal of Transportation Technologies*, **11**, 78-89. https://doi.org/10.4236/jtts.2021.111005

[10] Koudougou, S., Yonli, H., Sougoti, M. and Toguyeni, D. (2023) Thermal Effect of Braking on Pavements during Heat Waves in Ouagadougou. *Materials Sciences and Applications*, **14**, 382-396. https://doi.org/10.4236/msa.2023.147024

[11] Arora, S. and Vasudavan, S. (2017) Analysis of Sloshing Induced Load on Fuel Tank Structure. Master's Thesis, Chalmers University of Technology, Gothenburg.

[12] Memoire presente a l'université du Québec à chicoutimi comme exigence partielle de la maîtrise en ingénierie. https://central.bac-lac.gc.ca/.item?id=MR91633&op=pdf&app=Library&oclc_number=911213140

[13] El-Sharkawy, M. (2022) Difference between Mawp and Design Pressure. https://www.linkedin.com/pulse/difference-between-mawp-design-pressure-mohamed-el-sharkawy

[14] Clive Stone (2020) Understanding Maximum Allowable Working Pressure (MAWP).

[15] Koli, G.C. and Kulkarni, V.V. (2010) Simulation of Fluid Sloshing in a Tank. *Proceedings of the World Congress on Engineering* 2010, London, 30 June-2 July 2010, 1.

[16] Maleki, A. and Ziyaeifar, M. (2007) Sloshing Damping in Cylindrical Liquid Storage Tanks with Baffles. https://www.academia.edu/26589571/Sloshing_damping_in_cylindrical_liquid_storage_tanks_with_baffles

[17] COMSOL Multiphysics Model Library Manual. https://doc.comsol.com/5.5/doc/com.comsol.help.comsol/COMSOL_ReferenceManual.pdf

[18] Zheng, X.-L., Li, X.-S., Ren, Y.-Y., Wang, Y.-N. and Ma, J. (2013) Effects of Transverse Baffle Design on Reducing Liquid Sloshing in Partially Filled Tank Vehicles. *Green Transportation System and Safety*, **2013**, Article ID 130570. https://doi.org/10.1155/2013/130570

[19] Ren, L., Zou, Y.J., Tang, J.B., Jin, X., Li, D.S. and Liu, M.M. (2021) Numerical Modeling of Coupled Surge-Heave Sloshing in a Rectangular Tank with Baffles. *Advances in Prediction and Evaluation of Liquid Sloshing Dynamics*, **2021**, Article ID 5545635. https://doi.org/10.1155/2021/5545635

[20] Virella, J.C. and Suarez, L.E. (2005) Effect of Pre-stress States on the Impulsive Modes of Vibration of Cylindrical Tank-liquid Systems under Horizontal Motions. *Journal of Vibration and Control*, **11**, 1195-1220. https://doi.org/10.1177/1077546305057221

[21] Degtyarev, K., Gnitko, V., Naumenko, V. and Strelnikova, E. (2016) Reduced

Boundary Element Method for Liquid Sloshing Analysis of Cylindrical and Conical Tanks with Baffles. *International Journal of Electronic Engineering and Computer Science*, **1**, 14-27.